A TWO-DIMENSIONAL FINITE-ELEMENT MODEL STUDY OF BACKWATER AND FLOW DISTRIBUTION AT THE I-10 CROSSING OF THE PEARL RIVER NEAR SLIDELL, LOUISIANA

By Jonathan K. Lee, David C. Froehlich,

J. J. Gilbert, and Gregg J. Wiche

U.S. GEOLOGICAL SURVEY

Water-Resources Investigations Report 82-4119

Prepared in cooperation with the

LOUISIANA DEPARTMENT OF TRANSPORTATION

AND DEVELOPMENT, OFFICE OF HIGHWAYS,

and the UNITED STATES DEPARTMENT OF TRANSPORTATION,

FEDERAL HIGHWAY ADMINISTRATION

NSTL Station, Mississippi

1983

UNITED STATES DEPARTMENT OF THE INTERIOR

JAMES G. WATT, Secretary

GEOLOGICAL SURVEY

Dallas L. Peck, Director

For additional information write to:

U.S. Geological Survey, WRD
Gulf Coast Hydroscience Center
Building 2101
NSTL Station, MS 39529

Copies of this report can be purchased from:

Open-File Services Section
Western Distribution Branch
U.S. Geological Survey
Box 25425, Federal Center
Lakewood, CO 80225
(Telephone: (303) 234-5888)

CONTENTS

ILLUSTRATIONS

PLATES

TABLES

CONVERSION FACTORS

Factors for converting inch-pound units to the International System of Units (SI) are shown to four significant figures.

Multiply inch-pound unit	By	To obtain SI unit
foot (ft)	3.048×10^{-1}	meter (m)
foot to the one-sixth power ($ft^{1/6}$)	8.204×10^{-1}	meter to the one-sixth power ($m^{1/6}$)
foot to the one-half power per second ($ft^{1/2}/s$)	5.521×10^{-1}	meter to the one-half power per second ($m^{1/2}/s$)
foot per second (ft/s)	3.048×10^{-1}	meter per second (m/s)
foot per square second (ft/s^2)	3.048×10^{-1}	meter per square second (m/s^2)
cubic foot per second (ft^3/s)	2.832×10^{-2}	cubic meter per second (m^3/s)
mile (mi)	1.609	kilometer (km)
square mile (mi^2)	2.590	square kilometer (km^2)
foot per mile (ft/mi)	1.894×10^{-1}	meter per kilometer (m/km)
slug per cubic foot ($slug/ft^3$)	5.154×10^2	kilogram per cubic meter (kg/m^3)
pound second per square foot ($lb{\cdot}s/ft^2$)	4.787×10^2	pascal second (Pa•s)

National Geodetic Vertical Datum of 1929 (NGVD of 1929): A geodetic datum derived from a general adjustment of the first-order level nets of both the United States and Canada, called NGVD of 1929, is referred to as sea level in this report.

A TWO-DIMENSIONAL FINITE-ELEMENT MODEL STUDY OF BACKWATER AND FLOW DISTRIBUTION AT THE I-10 CROSSING OF THE PEARL RIVER NEAR SLIDELL, LOUISIANA

By Jonathan K. Lee, David C. Froehlich,
J. J. Gilbert, and Gregg J. Wiche

ABSTRACT

A two-dimensional finite-element surface-water flow modeling system based on the shallow-water equations was used to study the effect of Interstate Highway 10 (I-10) on water-surface elevations and flow distribution during the flood of April 2, 1980, on the Pearl River near Slidell, Louisiana. The model can be used to simulate both lateral and longitudinal velocities and variations in water-surface elevation, highly variable flood-plain topography and vegetative cover, and geometric features such as highway embankments, dikes, and channel bends. Geometric features of widely varying sizes are easily accommodated within a single finite-element network.

A finite-element network was designed to represent the topography and vegetative cover of the study reach. Hydrographic data collected for the April 1980 flood were used to calibrate the flow model. The finite-element network was then modified to represent conditions without I-10 in place, and the hydraulic impact of I-10 was determined by comparing results with and without I-10.

Model results show that, without I-10 in place, much of the flow shifts from the west side of the flood plain to the east side upstream from the site of I-10. With I-10 in place, this flow shift occurs somewhat farther upstream than it does without the roadway in place. Upstream from the roadway, maximum backwater at the west edge of the flood plain is 1.5 feet, and maximum backwater at the east edge is 1.1 feet, but backwater extends farther upstream along the east edge of the flood plain than along the west edge. Backwater ranging from 0.6 to 0.2 foot extends more than a mile downstream from the Pearl River bridge opening in I-10 at the east edge of the flood plain, and drawdown of 0.2 foot or more occurs along approximately 2 miles of the west edge of the flood plain downstream from I-10.

The capability of the modeling system to simulate the significant features of steady-state flow in a complex multichannel river-flood-plain system with variable topography and vegetative cover was successfully demonstrated in this study. These features included lateral variations in discharge distribution and backwater or drawdown.

INTRODUCTION

In April 1979 and April 1980, major flooding on the lower Pearl River caused extensive damage to homes located on the flood plain in the Slidell, La., area. Many persons were forced from their homes until the flood waters receded. Property damages in the Slidell area due to the 1980 flood, the largest flood of record in the area, were estimated to be $12.275 million (U.S. Army Corps of Engineers, 1981, p. 76). The 1980 flood forced the closing of the I-10 crossing of the Pearl River flood plain between Slidell and Bay St. Louis, Miss., for several hours while the flood crest passed. Many local residents attributed part of the 1979 and 1980 flooding in the Slidell area to backwater caused by the I-10 embankments.

The U.S. Geological Survey, in cooperation with the Louisiana Department of Transportation and Development, Office of Highways, and the U.S. Department of Transportation, Federal Highway Administration, undertook to determine the effect of the highway crossing on water-surface elevations and flow distribution during the April 2, 1980, flood for three reasons: (1) there was much interest in the impact of I-10; (2) the April 1980 flood was a large flood, which partially inundated the I-10 crossing; and (3) the study offered the opportunity to test a two-dimensional finite-element flow modeling system in a multichannel flood plain.

The two-dimensional finite-element surface-water flow modeling system FESWMS was used to study the effect of I-10 during the 1980 flood. The width of the Pearl River flood plain, constrictions created by highway embankments, and other physical features of the flood plain caused significant lateral variations in water-surface elevation and flow distribution during the 1980 flood. Thus, use of a two-dimensional model was warranted in order to obtain a more precise evaluation of water-surface elevations and flow distribution near the I-10 crossing than could be obtained by one-dimensional backwater and conveyance techniques.

An earlier version of the modeling system FESWMS was used to study the impact of a proposed highway crossing on flood stages of the Congaree River near Columbia, S.C. (Lee, 1980; Lee and Bennett, 1981). In the Congaree River study, it was demonstrated that the model can be used to simulate both lateral and longitudinal velocities and variations in water-surface elevation. Highly variable flood-plain topography and vegetative cover and geometric features such as highway embankments, dikes, and channel bends can be readily accounted for in a finite-element network. Moreover, geometric features of widely varying sizes are easily accommodated within a network. In order to demonstrate that FESWMS can be used effectively to analyze steady-state flow in large multichannel flood plains, the Geological Survey used the model to determine the effect of the I-10 crossing on water-surface elevations and flow distribution during the April 1980 flood on the Pearl River.

This report presents the application of FESWMS to the Pearl

River and illustrates the usefulness of the two-dimensional model in analyzing steady-state flow with both lateral and longitudinal variations. The report begins with a brief description of the modeling system FESWMS, a description of the study area, and a discussion of the hydrology of the Pearl River basin. Data collection, network design, and model adjustment for the 1980 flood with I-10 in place are described. Results of the simulation of the 1980 flood both with and without I-10 in place are presented, and backwater and drawdown caused by the roadway are discussed.

The assistance of the following individuals and organizations in making available data for this study is gratefully acknowledged: William T. Jack, Jr., Louisiana Department of Transportation and Development, Office of Highways; and Harold V. Doyal and Michael W. Peterson, U.S. Army Corps of Engineers, Mobile District. The support of the U.S. Department of Transportation, Federal Highway Administration, is also gratefully acknowledged. Computer work was done on an IBM 3033[1/] at Johns Hopkins University's Applied Physics Laboratory.

Throughout this report, the words "right" and "left" refer to positions that would be reported by an observer facing downstream. The words "backwater" and "drawdown" denote an increase and a decrease, respectively, in water-surface elevation caused by a flood-plain constriction. Backwater may occur both upstream and downstream from the constriction. Elevations refer to the National Geodetic Vertical Datum (NGVD) of 1929, called sea level in this report. A list of factors for converting inch-pound units to SI units is provided at the front of the report. All data supporting the conclusions of this report are available in the files of the Louisiana District office of the Geological Survey at Baton Rouge, La.

MODEL DESCRIPTION

The core of the modeling system FESWMS, which is under development by the Geological Survey, is a two-dimensional finite-element surface-water flow model based on the work of Norton and King (Norton and King, 1973; Norton and others, 1973; Tseng, 1975; King and Norton, 1978). Around this core, the Geological Survey has developed pre- and postprocessing programs which make the system accessible to the user. Preprocessing programs place input data in an appropriate form for the flow model and plot maps of finite-element networks and associated data. Postprocessing programs plot maps of velocity vectors, water-surface contour lines, lines of equal backwater and drawdown, discharge at specified cross sections, and observed high-water marks.

The formulation and development of the flow model have been reported elsewhere; therefore, only the equations solved and a brief outline of the technique used to solve them are presented here.

[1/]The use of brand names in this report is for identification purposes only and does not imply endorsement by the U.S. Geological Survey.

Flow Equations

Under the usual assumptions (for example, hydrostatic pressure and momentum correction factors of unity), two-dimensional surface-water flow in the horizontal plane is described by three nonlinear partial-differential equations, two for conservation of momentum and one for conservation of mass (Pritchard, 1971):

$$\frac{\partial u}{\partial t} + u\frac{\partial u}{\partial x} + v\frac{\partial u}{\partial y} + g\frac{\partial h}{\partial x} + g\frac{\partial z_o}{\partial x} - \frac{1}{\rho h}\left[\frac{\partial}{\partial x}\left(\varepsilon_{xx} h \frac{\partial u}{\partial x}\right) + \frac{\partial}{\partial y}\left(\varepsilon_{xy} h \frac{\partial u}{\partial y}\right)\right]$$

$$- 2\omega v \sin \varphi + \frac{gu}{C^2 h}(u^2 + v^2)^{1/2} - \frac{\zeta}{h} V_a{}^2 \cos \psi = 0, \qquad (1)$$

$$\frac{\partial v}{\partial t} + u\frac{\partial v}{\partial x} + v\frac{\partial v}{\partial y} + g\frac{\partial h}{\partial y} + g\frac{\partial z_o}{\partial y} - \frac{1}{\rho h}\left[\frac{\partial}{\partial x}\left(\varepsilon_{yx} h \frac{\partial v}{\partial x}\right) + \frac{\partial}{\partial y}\left(\varepsilon_{yy} h \frac{\partial v}{\partial y}\right)\right]$$

$$+ 2\omega u \sin \phi + \frac{gv}{C^2 h}(u^2 + v^2)^{1/2} - \frac{\zeta}{h} V_a{}^2 \sin \psi = 0, \qquad (2)$$

and

$$\frac{\partial h}{\partial t} + \frac{\partial}{\partial x}(uh) + \frac{\partial}{\partial y}(vh) = 0, \qquad (3)$$

where

- x, y = Cartesian coordinates in the positive east and north directions, respectively (feet),
- t = time (seconds),
- u, v = depth-averaged velocity components in the x- and y-directions, respectively (feet per second),
- h = depth (feet),
- z_o = bed elevation (feet),
- ρ = density of water (assumed constant) (slugs per cubic foot),
- ω = rate of the Earth's angular rotation (per second),
- ϕ = latitude (degrees),
- g = gravitational acceleration (feet per square second),
- C = Chézy coefficient (feet to the one-half power per second),
- $\varepsilon_{xx}, \varepsilon_{xy}, \varepsilon_{yx}, \varepsilon_{yy}$ = eddy viscosities (pound second per square foot),
- ζ = water-surface resistance coefficient (nondimensional),
- V_a = local wind velocity (feet per second), and
- ψ = angle between the wind direction and the x-axis (degrees).

The two-dimensional surface-water flow equations account for energy losses through two mechanisms: bottom friction and turbulent stresses. The Chézy equation for bottom friction in open-channel flow is extended to two dimensions for use in equations 1 and 2. Equations 1 and 2 also use Boussinesq's eddy-viscosity concept, which assumes the turbulent stresses to be proportional to the mean-velocity gradients.

Boundary conditions consist of the specification of flow components or water-surface elevations at open boundaries and zero flow components or zero normal flow (tangential flow) at all other boundaries, called lateral boundaries. For a time-dependent problem, initial conditions must also be specified. Equations 1 through 3, together with properly specified initial and boundary conditions, constitute a well-posed initial-boundary-value problem.

Numerical Solution of the Flow Equations

Quadratic basis functions are used to interpolate velocity components, and linear basis functions are used to interpolate depth on triangular, six-node, isoparametric elements (mixed interpolation). Model topography is defined by assigning a ground-surface elevation to each element vertex and requiring the ground surface to vary linearly within an element.

The finite-element model requires the specification of a constant Chézy coefficient, C, and a constant symmetric turbulent-exchange, or eddy-viscosity, tensor, ε, over each element. Nonisotropic turbulent stresses can be simulated by assigning different values to the components of the eddy-viscosity tensor. The eddy-viscosity terms in the momentum equations suppress nonlinear instabilities generated by the convective terms, and nonzero eddy-viscosity values are necessary for convergence of the numerical method to a solution. The eddy-viscosity values can influence the results of a simulation; however, optimum values are difficult to determine. In general, increased values serve to increase water-surface slopes. It is also known that eddy-viscosity values should increase with element size.

Flow components are specified at inflow boundary nodes, and water-surface elevations are specified at outflow boundary nodes. In this study, zero normal flow was specified at all lateral boundaries. Isoparametric elements permit the use of smooth, curved lateral boundaries. The improvement in accuracy obtained by using such boundaries, together with the specification of zero normal flow (tangential flow) there, has been documented by Gee and MacArthur (1978), King and Norton (1978), and Walters and Cheng (1978, 1980) for the mixed-interpolation formulation of the surface-water flow equations.

Galerkin's method of weighted residuals, a Newton-Raphson iteration scheme, numerical integration using seven-point Gaussian quadrature (Zienkiewicz, 1977, p. 200-201), and a frontal solution algorithm using out-of-core storage (Hood, 1976, 1977) are used to solve for the nodal values of the velocity components and depth. The time derivatives are handled by an implicit finite-difference scheme; in the application reported here, however, only the steady-state forms of the equations were solved.

If a finite-element network is not well designed, errors in conservation of mass can be significant because there are only approximately half as many equations for conservation of mass as there are for conservation of momentum in either the x- or y-direction. For a well-designed network, however, errors in mass conservation are small. The model has the capability of integrating the discharge across a line following element sides and beginning and ending at element vertices. Thus, conservation of mass can be checked (King and Norton, 1978).

The interested reader may consult the books by Pinder and Gray (1977) and Zienkiewicz (1977) for additional information on the finite-element method.

DESCRIPTION OF THE STUDY AREA

Pearl River Basin

The Pearl River basin is about 240 mi long and 50 mi wide. The basin drains a large part of Mississippi and part of southeastern Louisiana. The basin is bounded on the north by the Tombigbee River basin, on the east by the Pascagoula River basin, on the south by Lake Borgne and the Mississippi Sound, and on the west by the Mississippi River basin and several coastal streams in southeastern Louisiana. The basin lies within the Gulf Coastal Plain. Elevations within the basin range from sea level along the coast to about 650 ft above sea level in the north-central hills.

The Pearl River originates in Neshoba County, Miss., at the confluence of Nanawaya and Tallahaga Creeks. From its origin, it flows southwestward for 130 mi to the vicinity of Jackson, Miss., then southeastward for another 281 mi to empty into Lake Borgne. Most of the low-water flow of the Pearl is transferred to the West Pearl River through Holmes Bayou 28 mi above the West Mouth of the West Pearl at the Rigolets (fig. 1). Cardwell and others (1967, p. 43) have described this westward shift of flow:

> The bottom lands...are laced by cross-connecting channels which distribute flow across these bottoms during periods of high river stage. In the vicinity of Picayune, Miss., the main channel of the Pearl River begins to shift westward to become the West Pearl River. A small cross channel, Farr Slough, leaves the main channel near Picayune and joins Hobolochitto Creek. The channel, known downstream as the "Pearl River," begins at this confluence. There is evidence that this eastern channel was once the major channel of the lower Pearl River system and that a portion of the old channel near Picayune became filled when the flow shifted to the west... It is estimated that during times

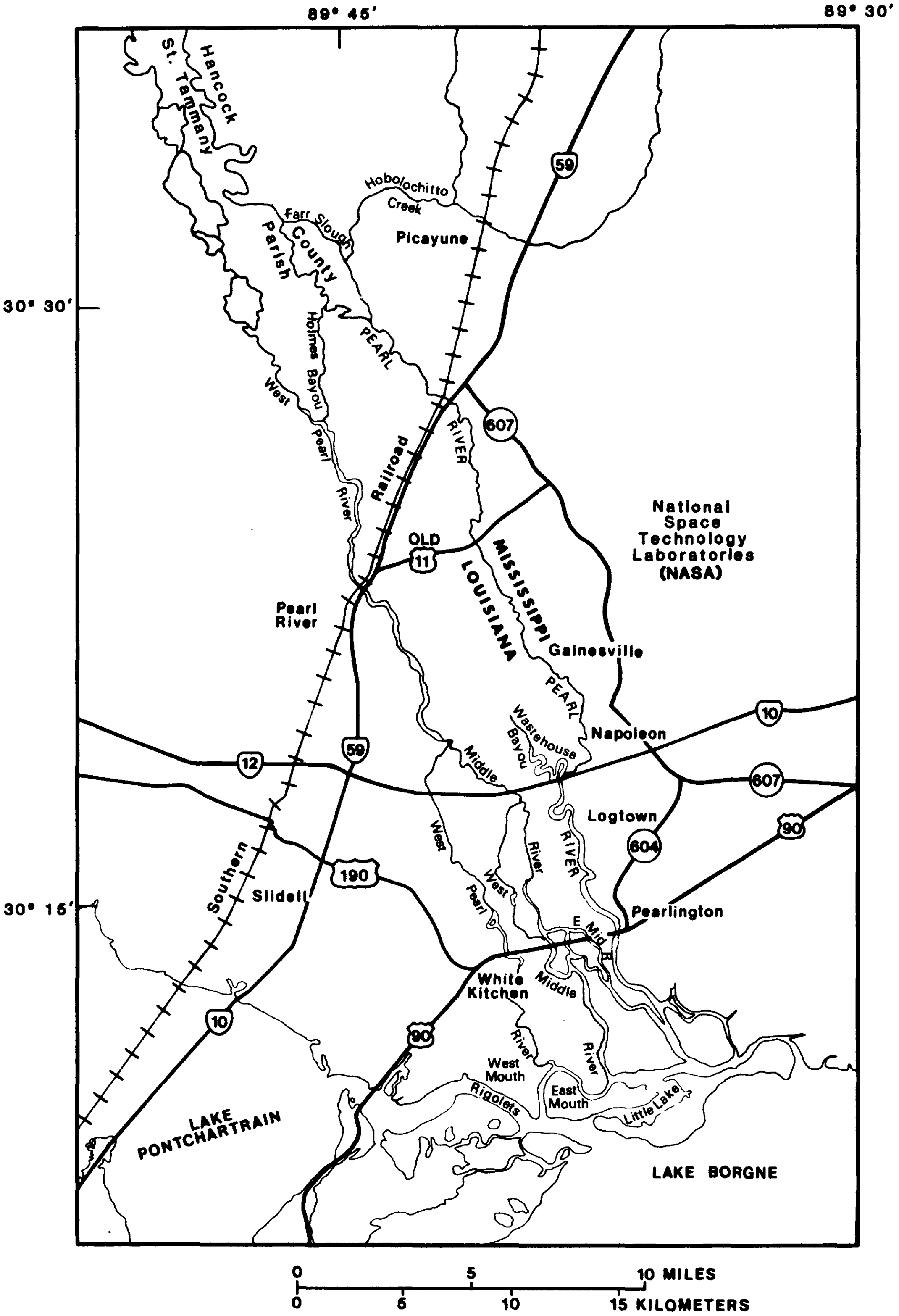

Figure 1.--Lower Pearl River basin, Louisiana and Mississippi.

of minimum flow in the system, less than 5 percent of the flow in the main channel flows through Farr Slough to continue in the eastern channel and the remainder flows through the western channel. At maximum flood stages there is considerable flow across the flood plain, and the eastern channel carries the greater part of the flow in the system.

From the confluence of Holmes Bayou and the West Pearl River, the main river channels continue generally southward and south-southeastward to the mouths of the Pearl River system. The Pearl River flows into Lake Borgne; the West Middle River, a distributary channel, and the East Mouth of the West Pearl River flow into Little Lake; and the West Mouth of the West Pearl River flows into the Rigolets (fig. 1). The drainage area of the Pearl Rivers is 8,670 mi^2 at the mouths of the system (Shell, 1981, p. 232).

The major tributaries to the Pearl River are Lobutcha and Tuscolameta Creeks and the Yockanookany, Strong, and Bogue Chitto Rivers. The main channel of the Pearl River has a slope of about 1 ft/mi and varies in width from about 100 to about 1,000 ft. The channel meanders within the flood plain and is obstructed in many places by sand bars, brush, and fallen and overhanging trees. The Ross Barnett Reservoir, put into operation in 1961, is located upstream from Jackson on the Pearl River and is the only major reservoir within the basin.

Study Reach

The reach of the Pearl River flood plain studied in this report is shown in figure 2. Ground-surface contour lines within the study area are shown on plate 1. The study reach is located in the lower part of the basin between river miles 9.0 and 26.3 on the Pearl River and river miles 7.9 and 21.9 on the West Pearl River. (River miles are defined for each of the channels modeled in detail in this study and are shown in fig. 2 and on all plates. In each case, river mile zero is defined as the channel mouth. The Geological Survey assigned all river miles except those for the West Pearl River, which were assigned by the Corps of Engineers.) The study reach, approximately 12 mi long, is bounded on the north by old U.S. Highway 11 and Interstate Highway 59 (I-59) and on the south by U.S. Highway 90. (Old Highway 11 is used only for access to the flood-plain forests because the bridge across the Pearl River has been destroyed.) The eastern and western boundaries are the natural bluffs at the edges of the flood plain, where ground-surface elevations rise abruptly to 15 to 25 ft above sea level in the northern part of the study reach and to 5 to 15 ft above sea level in the southern part. Within the study reach, the axis of the flood plain is aligned in a north-northwest-to-south-southeast direction, and the flood plain varies in width from about 3 to about 7 mi.

The major channels in the study reach are the Pearl (known locally as the East Pearl), East Middle, Middle, West Middle, and

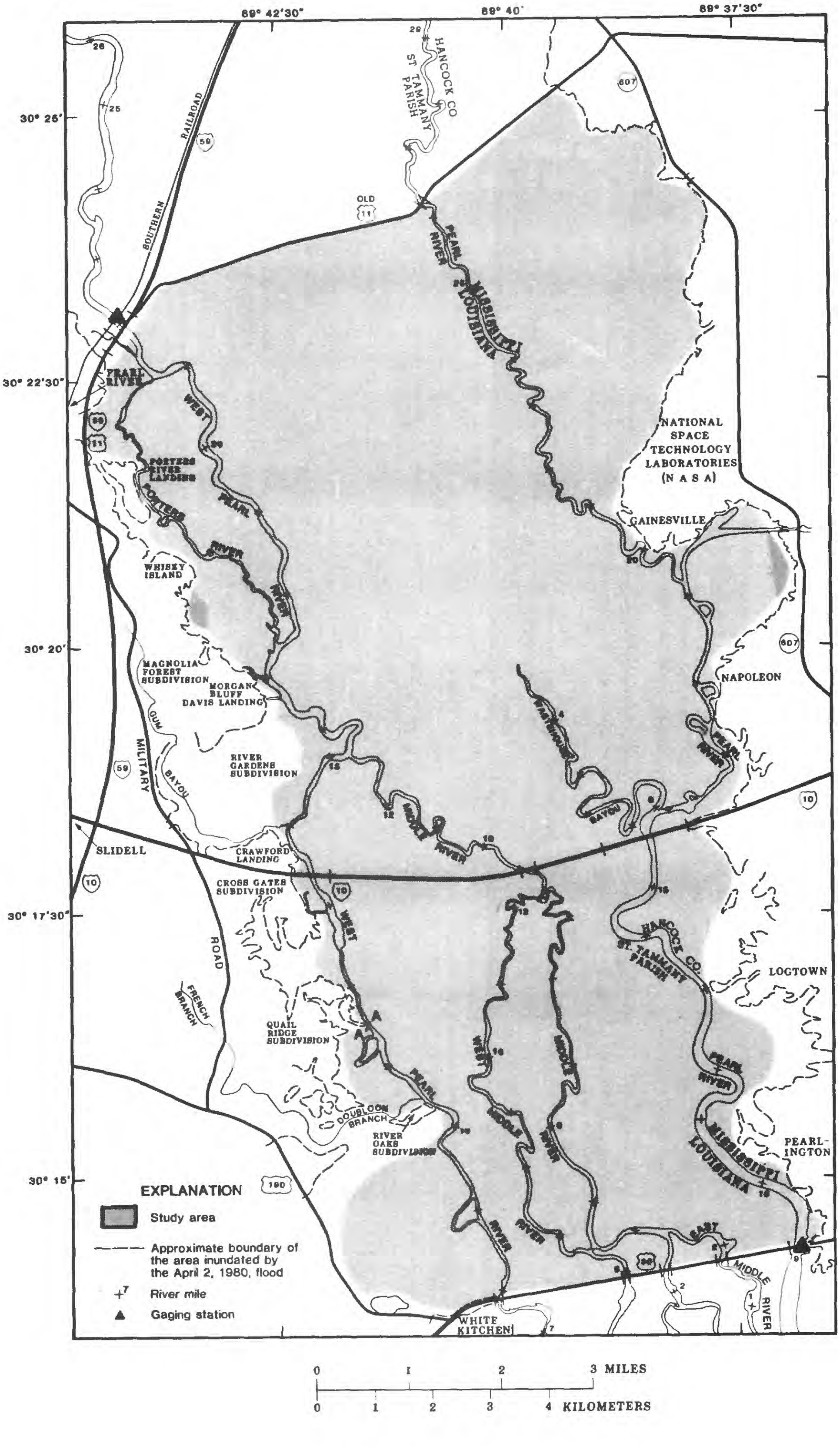

Figure 2.--Study reach of the lower Pearl River basin near Slidell. Cross section A-A' is shown in figure 6.

West Pearl Rivers, and Wastehouse Bayou. The Pearl flows along the east side of the flood plain, and the West Pearl along the west side. In the northern part of the study reach, the West Pearl is the largest channel in the flood plain. Near Gainesville, Miss., the channel of the Pearl becomes the largest and remains the largest to the mouths of the river system.

At river mile 15.2 on the West Pearl River, a distributary channel, the Middle River, forms and flows southeastward approximately 3.9 mi, where it divides into the Middle and West Middle Rivers. Approximately 6.3 mi farther south, the Middle River divides again, and another distributary channel, the East Middle River, forms. South of the study reach, the East Middle and Middle Rivers flow into the Pearl River about 1.3 mi north of Little Lake. Wastehouse Bayou forms within the flood plain and is tributary to the Pearl River just north of I-10.

There are numerous less significant channels in the flood plain within the study area. For example, Porters River, a branch of the West Pearl River, forms south of I-59 at river mile 21.4 and rejoins the West Pearl at river mile 17.4. Among the small streams which flow into the Pearl River system in the study reach are Gum Bayou and Doubloon Branch, which are tributary to the West Pearl River at river miles 14.0 and 10.5, respectively.

Flood-plain ground-surface elevations range from 1 ft above sea level in the southern part of the study area to 15 ft above sea level in the northwestern part. Between the upstream boundary and I-10, ground-surface elevations are higher near the West Pearl River than on the east side of the flood plain. Low natural levees border most of the channels in the study reach. The flood plain has a slope of about 1 ft/mi.

The streambeds and flood plain generally consist of alluvial soils and sands. The vegetative cover of the study area is shown on plate 1. Except near Highway 90, the flood plain is covered by dense woods, mixed with underbrush in many places. The flood-plain forests consist of bottomland hardwoods and bald-cypress tupelo-gum swamps. Near Highway 90, coastal marsh predominates, with dense grass 5 to 10 ft high. The taller grass borders the channels, and the shorter grass is found away from the channels. A small marsh area is located just downstream from the I-10 bridge across the Pearl River at the left edge of the flood plain.

Flow enters the study reach through the old Highway 11 bridge opening at the Pearl River, through the I-59 opening at the West Pearl River, and through numerous small openings in the old Highway 11 embankments. The I-59 opening at the West Pearl River is 2,630 ft long, and the old Highway 11 opening at the Pearl River is 570 ft long. The deck of the old Highway 11 bridge has been destroyed.

The I-10 crossing, about 4.4 mi long, spans the flood plain in an east-to-west direction in the middle of the study reach. There are bridges at the Pearl, Middle, and West Pearl Rivers, with lengths of 4,980, 770, and 2,240 ft, respectively. The embankment between the Pearl and Middle Rivers is about 0.8 mi long, and the embankment between the Middle and West Pearl Rivers is about 2.1 mi long. The embankments are about 300 ft wide, and the elevation of the roadway is between 12 and 13 ft above sea level.

Natural flood-plain elevations near I-10 range from 1 to 3 ft above sea level. Spoil from bridge construction increased these natural elevations by as much as 3 ft on the right overbank at the Pearl River bridge opening, by as much as 2 ft on both overbanks at the Middle River opening, and by as much as 6 to 7 ft on the left overbank at the West Pearl River opening. In addition, there is a large knoll adjacent to the southeast corner of the West Pearl River bridge that protrudes into the flow-expansion zone downstream from the bridge. This knoll was apparently created during construction of the highway embankments. The vegetation beneath the three bridges was removed during construction, but brush of varying density has grown back in the openings.

A short distance downstream from the West Pearl River bridge, between river miles 12.4 and 13.2, there is a relatively shallow reach of the West Pearl River, where the channel was artificially widened by the removal of earth fill during construction of the highway embankments.

Flow leaves the study reach through five openings in the Highway 90 embankments. The bridge at the Pearl River is 960 ft long; at the East Middle River, 630 ft long; at the Middle River, 580 ft long; at the West Middle River, 580 ft long, and at the West Pearl River, 570 ft long. During the April 1980 flood, there was a small amount of flow out of the study area over the top of the U.S. Highway 190 embankment.

HYDROLOGY OF THE PEARL RIVER BASIN

Flood Data

During the months of April 1979 and April 1980, extreme flooding on the Pearl River caused extensive property damage in subdivisions located on the flood plain in the Bogalusa (about 30 mi upstream from the study area) and Slidell, La., areas (fig. 3). Many persons were forced from their homes until the flood waters receded. The factors influencing the magnitude of these two floods have been discussed by Wax and Tingle (1980) and Lee and Arcement (1981).

The April 1979 flood was caused by heavy rainfall over the upper part of the basin, where as much as 19.6 in. of rain fell during one 2-day storm. This was the largest flood in the Jackson, Miss., area during the period of record (June 1901 to the current year, 1982) and the largest in the Bogalusa area during the period of record (October 1938 to the current year, 1982) (U.S. Geological Survey, 1981, p. 147; 1982, p. 23).

The April 1980 flood was caused by precipitation amounts

Figure 3.--Flooding near Slidell during April 1980. Upper photograph: Flooded homes. Lower photograph: Flooded business establishment. Photographs from the Slidell "Daily Times," 1980.

ranging from 8.6 to 15.0 in. over the entire Pearl River basin. This was the largest flood at Pearl River, La., near Slidell during the period of record (October 1899 to the current year, 1982). The approximately simultaneous arrival of the peak discharges of the Pearl and Bogue Chitto Rivers at their confluence caused a larger flood peak to occur near Slidell than would have been expected on the basis of the peak discharge recorded at Bogalusa. Urban property damage was estimated by the Corps of Engineers to be $12.275 million in the Slidell area alone (U.S. Army Corps of Engineers, 1981, p. 76). The April 1980 flood forced the closing of I-10 between Slidell and Bay St. Louis, Miss., for several hours while the flood crest passed (fig. 4).

Gage-height records have been collected at the Geological Survey gaging station, Pearl River near Bogalusa, La., from October 1938 to the current year, 1982. Water-surface elevations have ranged from about 59.8 to about 78.2 ft above sea level (April 24, 1979) during the 43-year period of record. At Bogalusa, maximum annual discharges between 1947 and 1981 have ranged in magnitude from 13,200 ft^3/s in 1952 to 129,000 ft^3/s in 1979 (April 24). (See U.S. Geological Survey, 1982, p. 23.)

Gage-height records have been collected at the Geological Survey gaging station, Pearl River at Pearl River, La. (fig. 2), from October 1899 to the current year, 1982. Water-surface elevations have ranged from about 1.5 to about 19.7 ft above sea level (from flood mark, April 1, 1980) during the 82-year period of record. A historical maximum of 20.2 ft above sea level occurred in 1874. At Pearl River, maximum annual discharges between 1947 and 1981 have ranged in magnitude from 17,700 ft^3/s in 1952 to 174,000 ft^3/s in 1980 (April 1). (See U.S. Geological Survey, 1982, p. 52.)

Gage-height records have been collected at the Corps of Engineers gaging station, Pearl River at Pearlington, Miss. (fig. 2), from December 1961 to the current year, 1982. Water-surface elevations have ranged from about 2.0 ft below to about 8.4 ft above sea level (September 10, 1965) during the 20-year period of record (U.S. Army Corps of Engineers, written commun., 1982). The maximum water-surface elevation during the April 1980 flood was 5.3 ft above sea level on April 2.

During the 1961, 1979, and 1980 floods, discharge measurements were made at or near peak flow at various highway crossings of the study reach. Each of these discharge measurements and the date it was made are given in table 1.

Approximately 200 high-water marks within and near the study area were located and flagged by the Geological Survey as the April 1980 flood waters receded. The Corps of Engineers ran a level loop around the study area to permit all high-water marks to be evaluated with respect to sea level. No high-water mark was located more than a mile from the nearest temporary bench mark on the level loop. Differential leveling from the temporary bench marks to the high-water marks was used by Geological Survey personnel to determine

Figure 4.--Overtopped north lane of I-10 between Slidell and Bay St. Louis during the April 2, 1980, flood.

Table 1.--Discharges measured during the 1961, 1979, and 1980 floods on the lower Pearl River

Date	Discharge, in cubic feet per second								
	I-59 bridge opening[1]								
	1 (Pearl River)	2	3	4	5	6	7	8 (West Pearl River)	Total
4-24-79	14,800	2,790	5,510	9,110	4,270	5,140	9,620	91,000	142,000
4-26-79	17,700	3,640	7,360	11,200	5,420	5,800	11,600	92,000	155,000

Date	I-10 bridge opening			
	Pearl River	Middle River	West Pearl River	Total
2-27-61	--	--	--	[2]106,000
4-26-79	88,600	29,000	33,800	151,000
5-01-79	55,000	16,600	18,700	90,000
4-02-80	103,000	30,000	40,800	174,000

Date	Highway 90 bridge opening					
	Pearl River	East Middle River	Middle River	West Middle River	West Pearl River	Total
4-22-80	51,900	11,800	16,700	16,600	6,830	104,000

1/The bridge openings are numbered from left to right as an observer faces downstream.
2/This measurement was made prior to the construction of I-10.

the elevations of the high-water marks. These elevations are accurate to within ±0.1 ft.

Flood Frequency

After the 1980 flood, the Geological Survey and the Corps of Engineers carried out a coordinated flood-frequency analysis for eight gaging stations on the Pearl River (U.S. Geological Survey, written commun., 1980). Discharges for specified recurrence intervals at two of these stations, Bogalusa and Pearl River, are given in table 2 (Lee and Arcement, 1981, p. 35). The values in the table were developed using procedures described by the U.S. Water Resources Council (1977). Skew values and historical flood data used in the analysis were mutually agreed upon by both agencies. The discharge of 174,000 ft^3/s measured at I-10 on April 2, 1980, is about 3 percent greater than the 50-year discharge at Pearl River.

SIMULATION OF THE APRIL 2, 1980, FLOOD

The two-dimensional finite-element surface-water flow modeling system FESWMS was used to determine the effect of I-10 on Pearl River flooding during the April 2, 1980, flood. Hydrographic and topographic data were collected and analyzed. These data were used to verify the assumption that a steady-state analysis is valid, define the region to be modeled, represent it as an equivalent finite-element network, and establish model boundary conditions. The initial finite-element network included the I-10 embankments. The hydrographic data were then used in calibrating the flow model to simulate the April 1980 flood as closely as possible.

Next, the finite-element network was modified to represent conditions without I-10 in place, and the hydraulic impact of I-10 was determined by comparing model results with and without I-10. Modeling the April 2, 1980, flood with the highway embankments in place is discussed in this section; modeling the flood without the embankments in place is discussed in the next section.

Data Collection and Analysis

A large amount of hydrographic and topographic data was collected and analyzed for use in modeling the April 2, 1980, flood. High-water marks recovered after the flood were examined for validity and grouped for use in establishing model boundary conditions and calibrating the model. Discharge measurements made by the Geological Survey and the Corps of Engineers at old Highway 11, I-59, I-10, and Highway 90 during the 1980 and earlier floods were assembled for the same purposes.

Detailed topographic information for the significant channels and their overbanks was obtained to ensure that model topography accurately represented prototype topography. A fathometer was used to obtain longitudinal profiles of the channels of the Pearl, East Middle, Middle, West Middle, and West Pearl Rivers, and Wastehouse

Table 2.--Flood frequency data for the Pearl River at Bogalusa and Pearl River

Station name	Drainage area, in square miles	Discharge, in cubic feet per second, for indicated recurrence interval, in years							
		2	5	10	25	50	100	200	500
Bogalusa	6,630	42,500	62,600	77,200	97,000	113,000	129,000	147,000	172,000
Pearl River.	8,590	56,500	87,400	111,000	143,000	169,000	198,000	228,000	272,000

Bayou, approximately 50 mi in all. Each profile was referenced in the field to outstanding topographic features.

On the basis of these profiles, sites were selected for 73 representative and special-purpose cross-section surveys needed to define channel geometry. A fathometer was used to establish channel-bottom elevations, and differential leveling with the water surface as a temporary benchmark was used to establish overbank elevations. The stadia method was used to measure distances. The water-surface elevation at a cross-section location was determined from upstream and downstream water-surface elevations established for the time that the cross section was being surveyed. During the time that this work was being done, flows were assumed steady except near Highway 90, where water-surface elevations were affected by tidal fluctuations of about 0.5 ft. Staff-gage readings were taken at frequent intervals, and the water-surface elevation at each cross section was adjusted for tidal fluctuations. Good control was maintained to ensure that computed water-surface elevations were accurate to within about ±0.25 ft.

Detailed topographic data at and near bridge openings were obtained from special topographic maps and highway-crossing plans provided by the Office of Highways. Additional field observations were made as the study progressed to describe conditions more adequately in problem areas. The collected data were supplemented by historic hydrologic data and Geological Survey topographic maps.

Infrared aerial photographs of the study area were obtained for use in determining vegetation type and density. Field observations of vegetation type and density were made to assist in estimating initial values of Chézy coefficients.

Steady-State Assumption

Water-surface elevations at the upper and lower ends of the study reach are plotted in figure 5 as a function of time for the period March 31 to April 4, 1980. These elevations were obtained from gage-height records at Pearl River and Pearlington. The peak water-surface elevation at Pearl River occurred before 6 a.m. on April 1, and the peak elevation at Pearlington occurred before midnight on April 2. At the time of the downstream peak, the upstream water-surface elevation had fallen less than 0.5 ft from its maximum value.

On the basis of this observation, it was assumed for modeling purposes that the flow was steady. This implies that the maximum discharge of 174,000 ft^3/s measured at I-10 was constant along the study reach and that all the high-water marks were attained by the water surface at the same time.

Network Design

The first task in applying the model to the April 2, 1980, flood was to define the boundaries of the area to be modeled and

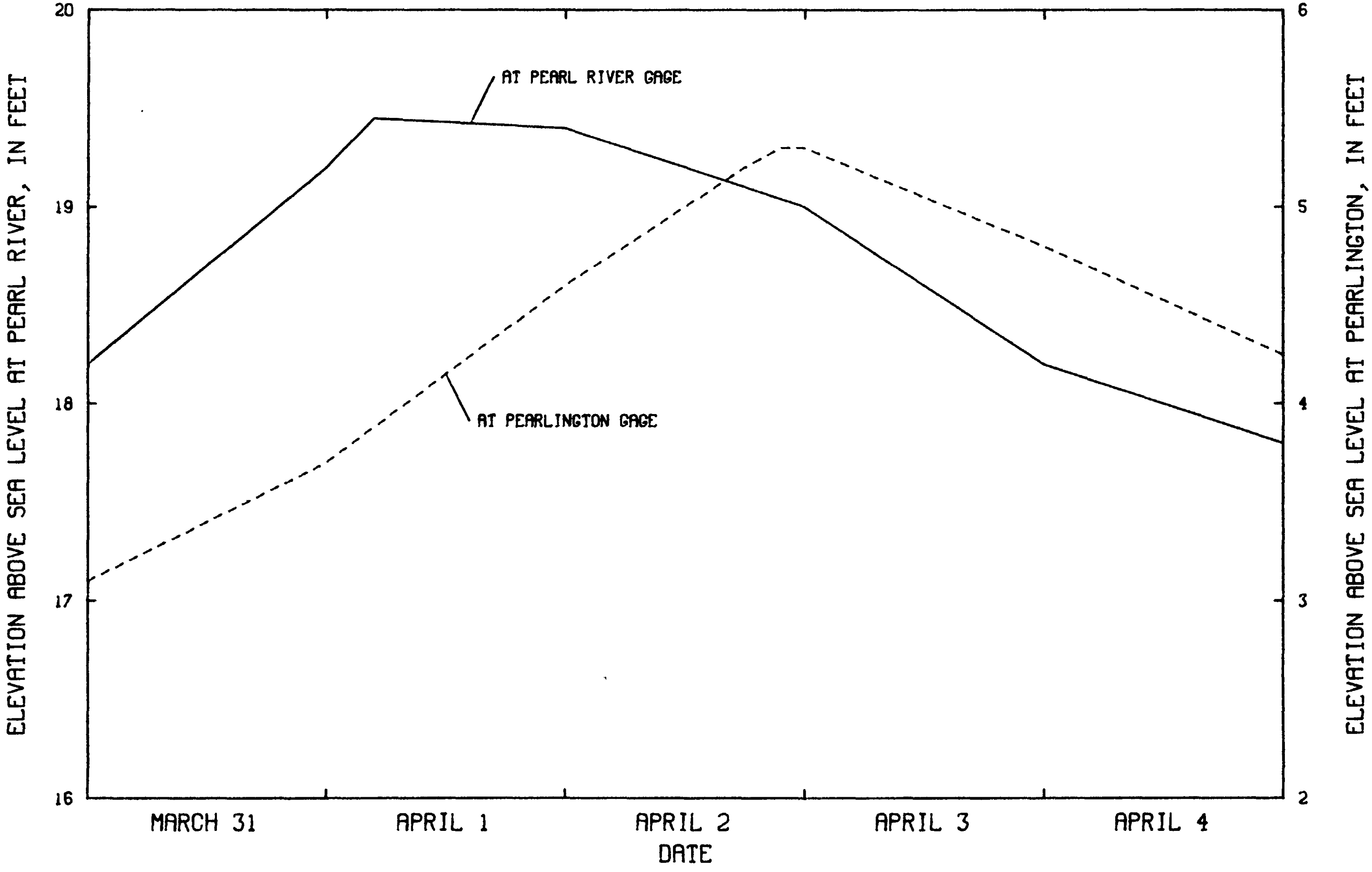

Figure 5.--Water-surface elevations at Pearl River and Pearlington from March 31 to April 4, 1980.

then represent the study area as an equivalent network of triangular elements. The finite-element network was prepared directly on Geological Survey topographic maps of the study area enlarged to a scale of 1 to 6,000.

The network, shown on plate 1, was designed to closely represent the highly nonuniform boundary of the area inundated by the 1980 flood. The upstream model boundary was located just downstream from and parallel to old Highway 11 and I-59, where inflows could be approximated on the basis of earlier discharge measurements. The downstream model boundary was located just upstream from and parallel to Highway 90, and outflows were placed at the five bridge openings, where water-surface elevations could be estimated on the basis of nearby high-water marks. Because both the upstream and downstream model boundaries were located at least one flood-plain width distant from the I-10 crossing, modifications made to the model near the highway crossing were assumed to have little effect on the boundary conditions. Smooth, curved-sided elements were used along all lateral boundaries, at which tangential flow was specified. The edges of the I-10 embankments and the adjoining knoll at the West Pearl River were also treated as tangential-flow boundaries.

After the boundaries were defined, the study area was subdivided into an equivalent network of triangular elements. Careful placement of nodes and elements was necessary to adequately represent prototype topography and vegetative cover. Subdivision lines between elements were located where abrupt changes in vegetative cover or topography occurred. Each element was designed to represent an area of nearly homogeneous vegetative cover.

It was found that water-depth changes of more than about 1,000 percent across an element often caused local inconsistencies in the solution. Occasionally, smaller depth changes caused problems. Hence, large prototype ground-surface gradients, such as those between over-banks and channel bottoms, required the use of additional network detail. In areas where velocity and water-surface gradients were expected to be relatively large, such as near bridge openings, network detail was increased to facilitate better simulation of the large gradients by the flow model. The use of curved-sided elements to define channel bends facilitated the design of a more realistic network.

The use of elements with aspect ratios greater than unity made it possible to design the network with fewer elements than would have been required otherwise. The element aspect ratio is defined as the ratio of the largest element dimension to the smallest. The optimum aspect ratio for a particular element depends largely on the local velocity and depth gradients. If these gradients can be estimated beforehand, it is possible to align the smallest element dimension with the largest variable change and the largest dimension with the smallest change.

Elements with large aspect ratios were used primarily in defining river channels. During network design, the longest element side was aligned with the channel axis, along which velocity and depth changes would typically be small. Element aspect ratios were kept to a maximum of about 10. In channel reaches with significant curvature, however, it was often necessary to use a much smaller value to avoid an unrealistic solution.

The complex geometry of the flood plain of the Pearl River was modeled in detail. Most prototype lengths and widths were realistically represented in the model; however, in order to reduce the number of elements in the finite-element network, several approximations were made. First, only relatively large channels, those of the Pearl, East Middle, Middle, West Middle, and West Pearl Rivers, and Wastehouse Bayou, were included in the network. Less important channels, such as Porters River, were not included in the model. Second, prototype channel cross sections were represented in the model by either triangular or trapezoidal cross sections with cross-sectional areas equal to the measured areas. A triangular model cross section and the prototype cross section to which it corresponds are shown in figure 6. Third, some meandrous channel reaches with relatively small flows were replaced with artificially straightened, but hydraulically equivalent, reaches (pl. 1). Hydraulic equivalence was obtained by decreasing the value of the Chézy coefficient of a straightened channel, as explained in detail on page 26. Lastly, the width of simulated stream channels was kept to a minimum of 200 ft.

Because of the large number of elements required to simulate prototype hydraulics accurately, the model was initially developed in three sections to reduce the cost of design and preliminary calibration. The study reach was divided approximately 2 mi above and 1 mi below I-10. The three sections of the network were designed simultaneously with coordinated effort. Estimated boundary conditions were used at the upstream and downstream boundaries of each of the sections to calibrate each of the sections on a preliminary basis. The three sections were then combined to perform final calibration and subsequent analysis.

In its complete state, the finite-element network contained a total of 5,224 triangular elements and 10,771 computational node points requiring the simultaneous solution of 23,697 nonlinear algebraic equations. The element areas ranged in size from 0.000116 to 0.438 mi^2 and covered a total area of 60.0 mi^2. Ground-surface elevations used in the model ranged from a minimum of 58.5 ft below sea level to a maximum of 15.0 ft above sea level.

Model Adjustment

After network design was complete, boundary conditions were determined, and the model was adjusted to simulate the April 2, 1980, flood as closely as possible.

Boundary Conditions

The discharge distribution at the upstream boundary (table 3) was based on the peak discharge of 174,000 ft^3/s measured at I-10

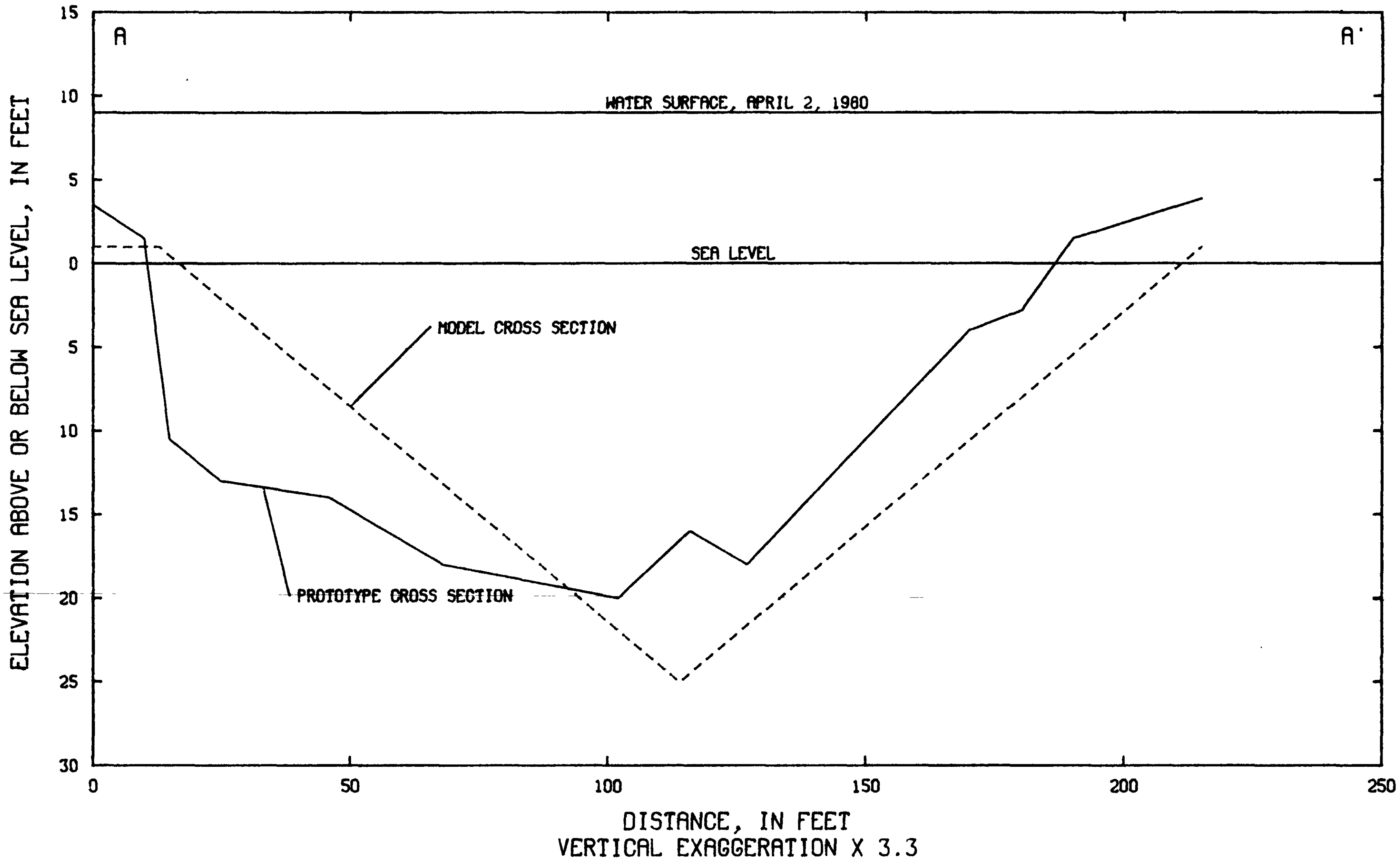

Figure 6.--Prototype and model channel cross sections at section A-A' (fig. 2).

Table 3.--Distribution of discharge at the upstream model boundary

Section of upstream boundary	Discharge, in cubic feet per second	Discharge, as percent of total discharge
Flood plain between east edge of flood plain and Pearl River.	22,100	12.7
Pearl River bridge opening	22,000	12.6
Flood plain between Pearl and West Pearl Rivers.	32,900	18.9
West Pearl River channel	69,100	39.7
Flood plain between West Pearl River and west edge of flood plain.	28,200	16.2
Total	174,000	100

and on previous discharge measurements at the bridge openings in old Highway 11 and I-59. Inflow was concentrated at the old Highway 11 bridge across the Pearl River and at the I-59 bridge across the West Pearl River. Flow into the study reach through numerous small openings in old Highway 11 was represented as continuous inflow between the east edge of the flood plain and the Pearl River and between the Pearl and West Pearl Rivers. Water-surface elevations at the downstream boundary (table 4) were based on high-water marks near the five bridge openings in Highway 90. Other minor inflows and outflows along the boundary of the modeled flood plain (for example, inflows from Gum Bayou and Doubloon Branch and outflow across Highway 190) were considered negligible and were not included in the simulation. In running each of the three network sections, intermediate downstream boundary conditions were estimated from nearby high-water marks, and intermediate upstream boundary conditions were obtained from the adjacent upstream section.

Aspects of Model Adjustment

The model-adjustment process consisted of two parts: the adjustment of empirical model coefficients (model calibration) and the adjustment of model boundary conditions, network detail, and ground-surface elevations on the basis of additional information obtained during the study.

The two-dimensional surface-water flow model is based on the formulation and solution of equations which simulate a complex physical flow situation. Since no physical flow system can be completely described or understood, the mathematical formulation involves some level of approximation. Three-dimensional topographic features are represented by two-dimensional elements, and the physics of flow is assumed to obey differential equations in which empirical hydraulic coefficients appear. Model calibration is the process of adjusting the values of the empirical coefficients so that the model simulates an observed flow as closely as possible. In this study, model calibration, performed by trial and error, was based on observed high-water marks and discharges obtained during the April 2, 1980, flood. This aspect of model adjustment will be discussed in detail.

The second aspect of the model-adjustment process involved the correction of deficiencies in the model boundary conditions and the representation of flood-plain topography. Although extensive data-collection work was done earlier, there were gaps in the data used to estimate model boundary conditions, design the model network, and assign model ground-surface elevations. During model adjustment, it occasionally became apparent that these data gaps were causing the model to fail to simulate correctly certain observed features of the 1980 flood. A review of existing data or additional data collection was necessary in these instances. Then boundary conditions, network detail, or ground-surface elevations were adjusted on the basis of the additional information. This aspect of model adjustment also will be discussed in detail.

Table 4.--Water-surface elevations at the downstream model boundary

Highway 90 bridge opening	Water-surface elevation above sea level, in feet
Pearl River	5.8
East Middle River	5.7
Middle River	5.7
West Middle River	5.8
West Pearl River	5.9

Preliminary Model Calibration

On the basis of previous finite-element simulations, the values of all components of the eddy-viscosity tensor were initially set at 100 lb·s/ft^2 for all elements in the network. Numerical experiments indicated that once the values of these coefficients were set high enough to ensure convergence, the solution was much less sensitive to changes in their values than to changes in the values of the Chézy coefficients. Because of a lack of information about their correct values and to avoid convergence problems, the values of all components of the eddy-viscosity tensor were maintained at 100 lb·s/ft^2 throughout the study for all elements in the network.

Once the values of the eddy viscosities were fixed, preliminary calibration work focused on determining the values of Chézy coefficients. Nominal values were selected for initial use with each of the three separate network sections on the basis of the infrared aerial photographs of the flood plain and field inspection. In making both the initial estimates of the Chézy values and subsequent modifications to them, care was taken to ensure that the assigned values were reasonable and mutually consistent. Areas to which different Chézy values were assigned are shown on plate 1, and the final values are given in table 5.

The Chézy value assigned to a channel element in an artificially straightened reach was derived from the value for the corresponding natural or unstraightened reach on the basis of the equation

$$C_s = C_n \sqrt{\frac{L_s}{L_n}}\,, \tag{4}$$

where C is the value of the Chézy coefficient (feet to the one-half power per second), L is the length of the reach (feet), and the subscripts s and n denote straightened- and natural-channel-reach values, respectively. Equation 4 is obtained directly from the Chézy equation.

A series of simulations with each of the three network sections was conducted to determine the relative effect on water-surface elevations of changes in the values of the Chézy coefficients of both overbank and channel elements. Computed water-surface elevations were most sensitive to changes in the value of the Chézy coefficient of the wooded flood plain. Changes in the Chézy values of channel elements had little or no effect on computed water-surface elevations except for channel reaches carrying a significant percentage of the total flow. Such reaches included the Pearl River between I-10 and Highway 90 and reaches located a few thousand feet upstream and downstream from bridge openings. Computed water-surface elevations were also moderately sensitive to the values of the Chézy coefficients of the overbank areas under the three I-10 bridges.

Table 5.--Values of Chézy coefficients used to simulate the April 2, 1980, flood

Element description or location	Chézy coefficient[1/] ($ft^{1/2}/s$)
Flood plain	
Woods	22
Low marsh grass in southern part of study reach	35
High marsh grass in southern part of study reach	28
Marsh grass and brush downstream from I-10 bridge across Pearl River.	30
Brush and trees south of preceding marsh-grass area	21
Grass and scattered brush on left overbank under I-10 bridge across Pearl River.	40 (22)
Grass and brush on right overbank under I-10 bridge across Pearl River.	30 (22)
Brush and trees under I-10 bridge across Middle River	21 (22)
Grass and scattered brush under I-10 bridge across West Pearl River.	40 (22)
Pearl River	
Natural channel between river miles 9.0 and 15.9	105
Natural channel between river miles 15.9 and 19.2	85
Straightened channel between river miles 19.2 and 20.3	[2/]85
Natural channel between river miles 20.3 and 20.9	85
Straightened channel between river miles 20.9 and 26.3	[2/]85
Wastehouse Bayou	
Straightened channel between river miles 0.0 and 4.4	59

Table 5.--Values of Chézy coefficients used to simulate the April 2, 1980, flood --Continued

Element description or location	Chézy coefficient[1/] ($ft^{1/2}/s$)
East Middle River	
Natural channel between river miles 1.8 and 2.7	85
Middle River	
Natural channel between river miles 2.3 and 5.4	85
Straightened channel between river miles 5.4 and 9.0	66
Natural channel between river miles 9.0 and 10.0	85
Straightened channel between river miles 10.0 and 12.9	68
West Middle River	
Natural channel between river miles 5.9 and 8.0	85
Straightened channel between river miles 8.0 and 12.7	75
West Pearl River	
Natural channel between river miles 7.9 and 14.9	85
Straightened channel between river miles 14.9 and 15.9	51
Natural channel between river miles 15.9 and 19.4	100
Straightened channel between river miles 19.4 and 20.4	94
Natural channel between river miles 20.4 and 21.4	100
Natural channel between river miles 21.4 and 21.9	115

[1/]Values in parentheses were used in the simulation without I-10 in place.
[2/]No correction factor was applied to the value of the Chézy coefficient for this straightened reach of the Pearl River.

Preliminary calibration consisted of matching as closely as possible all observed high-water marks as well as measured discharges at the three bridge openings in I-10.

Adjustment of Model Boundary Conditions, Network Detail, and Ground-Surface Elevations

Appropriate adjustments to the values of the Chézy coefficients gave close agreement between computed and observed data in most cases. In several areas, however, discrepancies between model results and observations made it necessary to obtain additional data or review previously obtained data. Additional field work was occasionally necessary to check the location and elevation of high-water marks and study previously overlooked topographic features. On the basis of the results of the early simulations and the additional observations, modifications were made to model boundary conditions, network detail, and model ground-surface elevations.

The upstream inflow at the West Pearl River was initially estimated by linear extrapolation of the discharge measured there on April 26, 1979, under the assumption that the percentage of the total discharge at the West Pearl opening was the same in 1979 and 1980 (table 1). A discharge of 103,000 ft^3/s was calculated by this procedure and used in early simulations with the upper model section. Inflows across the remaining sections of the upstream boundary were estimated on the basis of the April 26, 1979, discharge measurements at I-59 and earlier measurements at old Highway 11. With the resulting discharge distribution, the computed water-surface elevation was much higher than high-water-mark elevations near the West Pearl River bridge at location 1 (pl. 2, sheet 1) for any reasonable choice of the values of the Chézy coefficients.

A comparison of discharge measurements made on April 24 and April 26, 1979, indicates that the percentage of flow through the I-59 opening at the West Pearl River decreases as the total discharge increases (table 1). On the basis of this observation and to improve the agreement between the computed and observed water-surface elevations near the West Pearl opening in I-59, the model discharge there was decreased to 97,300 ft^3/s. Inflows across the rest of the upstream boundary were increased to maintain a total discharge of 174,000 ft^3/s. The final values for the different sections of the upstream boundary are given in table 3. Lowering the discharge at the West Pearl River opening improved the computed water-surface elevation at location 1 but still did not give adequate agreement between the computed and observed values.

During this adjustment, it was observed that computed water-surface elevations along the upstream boundary were quite sensitive to changes in the upstream discharge distribution. This sensitivity decreased rapidly with distance downstream. For example, as a result of the change discussed previously, the water-surface elevation at the upstream boundary increased by more than 0.2 ft in the Pearl River and decreased by more than 0.3 ft in the West Pearl

River. Less than 3 mi downstream, the maximum increase in water-surface elevation in the Pearl River was less than 0.05 ft, and the maximum decrease in the West Pearl River was less than 0.1 ft.

During the effort to identify the causes of the disagreement between the computed and observed water-surface elevations at location 1, a short earthen dike was discovered along the left bank of the West Pearl River approximately 0.1 mi downstream from I-59. The error at location 1 was caused in part by the omission of this dike from the original finite-element network. The inclusion of the dike in the network resulted in satisfactory agreement between the computed and observed water-surface elevations at location 1.

In early simulations, a lack of agreement was noted between the computed and observed discharges at the three I-10 bridge openings. Additional field observations indicated that the ground-surface elevations of the overbank areas within the highway right-of-way at the three I-10 bridge openings had been increased by the addition of fill during construction. Also, a check of the topographic data showed that flood-plain ground-surface elevations for about 2 mi upstream from the highway embankment between the Middle and West Pearl Rivers had been set 1 to 2 ft too high in the model. Correcting model ground-surface elevations at and near I-10 resulted in a better discharge distribution at I-10. In particular, decreasing the flood-plain ground-surface elevations upstream from the bridge opening at the West Pearl River increased the computed discharge at that opening.

Final Model Calibration

When satisfactory agreement between simulated and observed water-surface elevations and discharges was obtained, the three network sections were combined, and further calibration was performed. Minor adjustments to the values of the Chézy coefficients were needed for final calibration of the full-reach model. The final Chézy values were 22 $ft^{1/2}/s$ for the wooded flood plain, 28 to 35 $ft^{1/2}/s$ for the marsh-grass areas, 21 to 40 $ft^{1/2}/s$ for the overbank areas under the three I-10 bridges, and 85 to 115 $ft^{1/2}/s$ for the unstraightened channels. A more detailed listing of the final values of the Chézy coefficients is given in table 5. Computed element-averaged flow depths range from 2 to 23 ft for the wooded flood plain, from 4 to 10 ft for the marsh-grass areas, from 4 to 9 ft for the overbank areas under the I-10 bridges, and from 5 to 47 ft for the unstraightened channels. On the basis of these depths and the well-known relationship between the Manning roughness coefficient, n, and the Chézy coefficient (Chow, 1959, p. 100), Manning values corresponding to the final Chézy values are found to range from 0.077 to 0.114 $ft^{1/6}$ for the wooded flood plain, from 0.055 to 0.074 $ft^{1/6}$ for the marsh-grass areas, from 0.046 to 0.098 $ft^{1/6}$ for the overbank areas under the I-10 bridges, and from 0.021 to 0.033 $ft^{1/6}$ for the unstraightened channels.

In both this and earlier applications of FESWMS, the values of the Manning n required for model calibration are generally somewhat smaller than the values required to calibrate a one-dimensional model of the same reach. Several factors contribute to this situation. Wherever lateral flow is significant, streamlines are not parallel to the axis of the flood plain. Thus, flow paths are generally longer in a two-dimensional model than in a one-dimensional model, and it is possible to account for a given loss of energy with a smaller roughness coefficient than is needed in a one-dimensional model. In addition, some energy loss is accounted for by the turbulent-stress terms in the two-dimensional momentum equations. This loss must be accounted for by bottom friction in a step-backwater analysis.

Computed flow depths in the calibrated model average about 21 ft in the channels and about 8 ft on the flood plain. Most cross-sectional average channel velocities are between 1 and 3 ft/s. Somewhat higher velocities occur at several of the bridge openings. The average velocity on the flood plain is about 0.7 ft/s.

Comparison of Computed and Observed Water-Surface Elevations and Discharges

How well the model reproduces an observed flow depends on the approximations made in the model and on the calibration data. Calibrated model results represent a best fit to the available calibration data.

Network design and adjustment is a process of approximating hydraulically important topographic and vegetative-cover features with a finite number of homogeneous elements. The quality of the approximation depends on the amount and quality of the available topographic and vegetative-cover data. Further approximations are made in assigning model boundary conditions. In addition, the model equations describe the prototype flow process in an approximate way. The quality of this approximation depends in part on how well such assumptions as steady flow and the eddy-viscosity concept reflect prototype conditions. This approximation also depends on the values of the model's empirical coefficients, determined during calibration. Hence, velocities and water-surface elevations obtained from the calibrated model are approximate values, responses of approximate equations to approximate boundary conditions, topography, and vegetative cover.

Realistic and mutually consistent values of empirical parameters are chosen during calibration to bring model results into as close agreement as possible with observed data. If there is a major discrepancy between model results and observed data, then the approximations made in constructing the model are in error or the observed calibration data are not accurate or are not representative of the general hydraulic situation. The capability of a model to reproduce observed flows and subsequently predict the outcome of future or hypothetical flows depends largely on the amount and quality of the topographic, vegetative-cover, boundary-condition, and calibration data that are available. Thus, improvements in observed data can lead to more accurate simulation.

Plate 2 is a plot of the velocity field and water-surface contour lines for the calibrated model. Points lying on a specific water-surface contour line were located by interpolation between nodal water-surface elevations. The contour line was then obtained by drawing a smooth curve through the points. The locations of the high-water marks used in calibration are also shown on plate 2. Table 6 contains a list of the location reference numbers, computed water-surface elevations, observed high-water-mark elevations, and differences between the computed and observed elevations.

At many of the locations listed in table 6, several high-water marks were observed. In general, hydrologic field data reflect the dominant features simulated by the model; however, they also reflect local variation that is not represented in the model. For this reason, several observations of water-surface elevation near a particular location, giving a range of values or an average value, are more useful than a single observation for model calibration.

At most of the locations shown on plate 2, the computed water-surface elevation is in close agreement with the elevation of the observed high-water mark or marks at that location. It is not possible to determine how much of the difference between the computed and observed water-surface elevations is due to model error and how much is due to error in the elevations of the high-water marks. The mean absolute difference between the computed and observed values is 0.12 ft, and the root mean square difference is 0.18 ft. (Because the marks at locations 19, 20, and 21 were used to establish downstream boundary conditions, they were not used in computing the mean differences.) The computed water-surface elevations are within ± 0.3 ft of the elevations of the high-water marks at all but four locations, and at these four locations, the computed elevations are within ± 0.5 ft of the observed values.

The discharge measurements made at the I-10 bridge openings on April 2, 1980, were also used in model calibration. The computed and measured discharges for the left overbank, the channel, and the right overbank at each of the three openings are given in table 7. The computed discharges given in table 7 were obtained from continuity checks along the line of nodes closest to the south edge of the eastbound lane, where the measured discharges were obtained. The errors in computed discharge at the bridge openings at the Pearl, Middle, and West Pearl Rivers, as a percent of the measured discharge at each opening, are 7, -10, and -7, respectively. The sum of the computed discharges at the three openings is 175,000 ft^3/s. The cause of the small discrepancy between the total computed discharge at I-10 and the total upstream inflow is discussed on page 6. (Continuity checks were used to compute the total discharge at numerous cross sections along the study reach. The maximum difference between the computed discharge and the inflow is about 6 percent of the inflow.)

Table 6.--Elevations of the computed water surface and observed high-water marks for the April 2, 1980, flood

Location reference number[1/]	Elevation above sea level of computed water surface, in feet	Elevation above sea level of observed high-water mark(s)[2/], in feet	Computed water-surface elevation minus observed high-water mark[3/], in feet
1	18.5	17.9 - 18.0 (3)	0.5
2	17.4	17.2 (3)	0.2
3	16.6	16.7 (2)	-0.1
4	16.6	16.4 (2)	0.2
5	15.8	15.6 (1)	0.2
6	15.7	15.4 (1)	0.3
7	15.3	15.7 - 15.8 (2)	-0.4
8	15.2	15.2 (3)	0.0
9	15.1	15.0 - 15.1 (3)	0.0
10	13.4	13.5 (1)	-0.1
11	13.1	13.1 - 13.2 (2)	0.0
12	12.3	12.2 - 12.3 (3)	0.0
13	12.0	11.8 - 11.9 (4)	0.1
14	10.9	10.8 - 10.9 (6)	0.0
15	9.2	8.9 (1)	0.3
16	9.4	9.4 (1)	0.0
17	8.7	8.6 - 8.7 (2)	0.0
18	6.2	6.2 (1)	0.0
19	5.7	[4/]5.7 (1)	0.0
20	5.8	[4/]5.8 (1)	0.0
21	5.8	[4/]5.8 (1)	0.0

Table 6.--Elevations of the computed water surface and observed high-water marks for the April 2, 1980, flood--Continued

Location reference number[1]	Elevation above sea level of computed water surface, in feet	Elevation above sea level of observed high-water mark(s)[2], in feet	Computed water-surface elevation minus observed high-water mark[3],
22	7.3	7.1 (1)	0.2
23	7.1	6.9 (1)	0.2
24	7.5	7.3 (1)	0.2
25	7.7	7.4 (1)	0.3
26	8.3	8.2 (1)	0.1
27	8.6	8.6 (1)	0.0
28	8.6	8.4 (1)	0.2
29	8.6	8.6 (1)	0.0
30	8.6	8.5 (3)	0.1
31	11.6	11.1 - 11.2 (2)	0.4
32	11.8	11.6 - 11.9 (5)	0.0
33	12.6	12.4 - 12.7 (4)	0.0
34	12.8	12.4 - 12.8 (3)	0.0
35	12.8	12.8 - 12.9 (4)	0.0
36	14.1	14.1 - 14.3 (4)	0.0
37	14.7	14.7 - 14.8 (2)	0.0
38	15.7	15.2 - 15.6 (3)	0.1
39	11.8	11.5 - 11.6 (4)	0.2
40	11.8	11.7 (1)	0.1
41	10.3	10.1 - 10.5 (2)	0.0
42	12.7	12.5 - 12.8 (3)	0.0

Table 6.--Elevations of the computed water surface and observed high-water marks for the April 2, 1980, flood--Continued

Location reference number[1]	Elevation above sea level of computed water surface, in feet	Elevation above sea level of observed high-water mark(s)[2], in feet	Computed water-surface elevation minus observed high-water mark[3],
43	10.0	12.5 - 12.8 (3)	0.0
44	12.7	12.7 - 12.8 (4)	0.0
45	10.0	10.3 (3)	-0.3
46	12.6	12.6 - 12.7 (3)	0.0
47	10.5	10.8 - 10.9 (2)	-0.3
48	12.2	11.5 - 11.8 (2)	0.4

[1]Location reference numbers are shown on plate 2.
[2]The number of marks at a location is given in parentheses.
[3]The observed value nearest the computed value is used in computing the difference.
[4]This high-water mark was used to establish downstream boundary conditions and was not used in computing the mean differences.

Table 7.--Computed and measured discharges at the I-10 bridge openings

Opening section	Computed discharge, in cubic feet per second	Measured discharge, in cubic feet per second
	Pearl River	
Left overbank	23,600	21,500
Channel	50,200	52,000
Right overbank	36,100	29,600
Total	110,000	103,000
	Middle River	
Left overbank	3,810	1,920
Channel	17,800	20,400
Right overbank	5,360	7,670
Total	27,000	30,000
	West Pearl River	
Left overbank	10,000	11,300
Channel	16,900	19,700
Right overbank	11,000	9,800
Total	37,900	40,800

Discharge per unit distance or unit discharge, both computed and measured, is plotted as a function of distance at each of the three bridge openings in figures 7, 8, and 9. At each opening, the computed profile is shown along the line of nodes used to compute the discharges given in table 7. In general, there is good agreement between the computed and observed profiles, especially for the overbank areas. The profiles based on field observations are more variable than the computed profiles due to debris, flow around piers and fenders, and local variations in topography and vegetative cover. Because the main-channel fenders at the Pearl and West Pearl Rivers were not modeled in this study, the peak unit discharges at those openings are underestimated by the model.

Additional Results of the Simulation

The water-surface contour lines and the velocity field, shown on plate 2, together with the continuity checks used at numerous locations along the study reach, give additional information about water-surface elevations and flow distribution for the April 2, 1980, flood. Computed water-surface elevation is plotted as a function of river mile for the channels of the Pearl and West Pearl Rivers in figures 10 and 11, respectively. In addition, computed water-surface elevation is plotted for the east and west edges of the flood plain in figures 12 and 13, respectively. (As one moves downstream along either edge of the flood plain, there are short sections where the north-south coordinate increases rather than decreases due to the meandering boundary of the flood plain. This causes the multivalued behavior of the graphs plotted in figures 12 and 13.)

Between the upstream boundary and I-10, there is a movement of water from the west to the east side of the flood plain. At the upstream boundary, 56 percent of the inflow was estimated to pass through the bridge opening at the West Pearl River (table 3), but at I-10, 63 percent of the computed discharge passes through the bridge opening at the Pearl River (table 7). (Table 1 shows that 59 percent of the measured discharge passed through the Pearl River opening at I-10.) The velocity field in this reach is aligned in a generally southeastward direction.

The 15.5- to 20.5-foot water-surface contour lines (pl. 2, sheet 1) form a "mound" downstream from the I-59 bridge opening at the West Pearl River. At the upstream boundary, the water surface is more than 3 ft higher on the west side of the flood plain than on the east side. Downstream from the West Pearl River bridge opening, the water surface drops sharply both in the downstream direction and towards the east side of the flood plain. However, 2 mi downstream, the water surface remains 1 ft higher on the west side of the flood plain than on the east side. Between 3 and 4 mi downstream, the alignment and spacing of the contour lines, as well as the direction and magnitude of the velocity vectors, indicate that the flow has become uniformly distributed across the flood plain and parallel to the flood-plain axis.

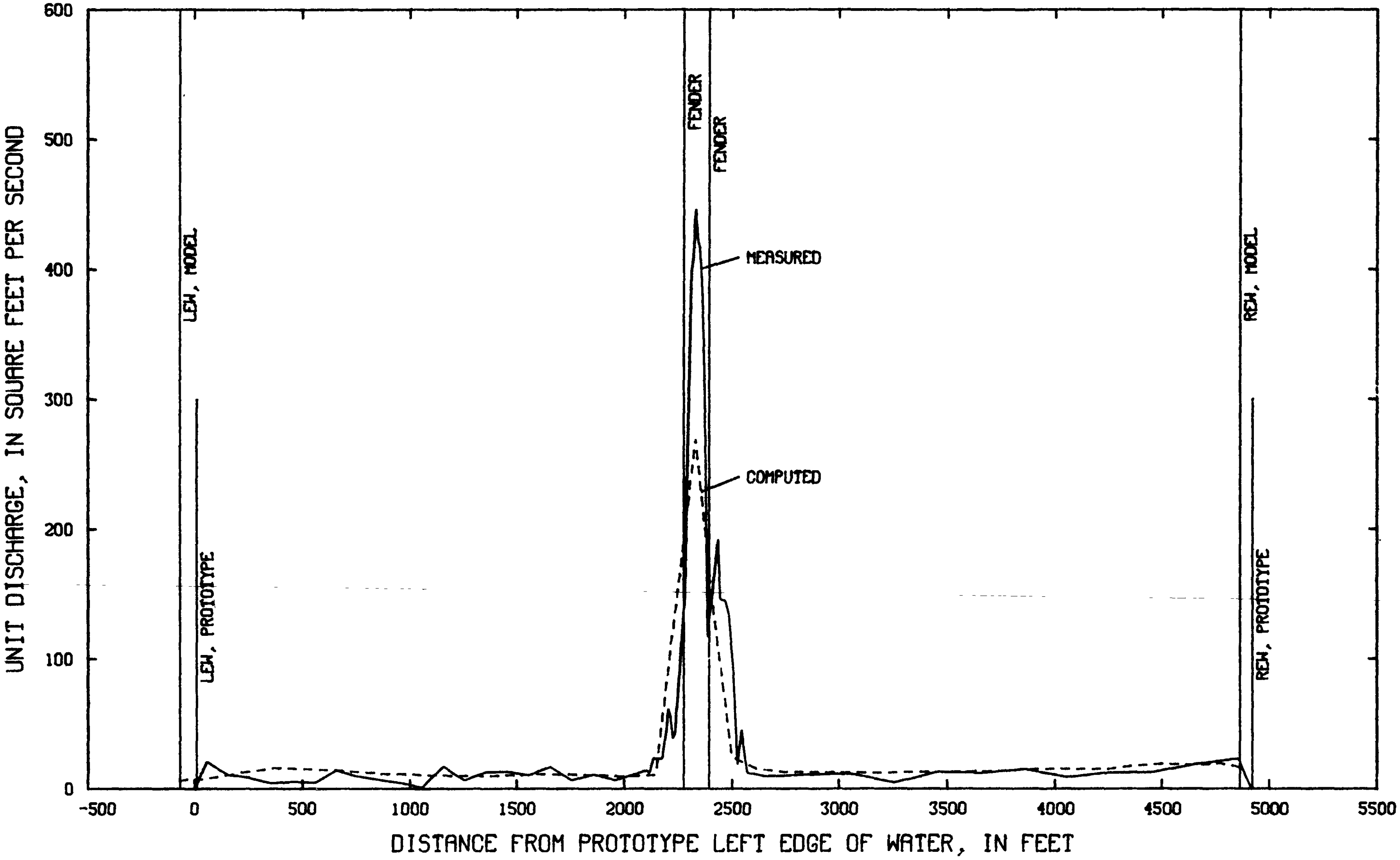

Figure 7.--Computed and measured unit discharge at the I-10 bridge opening at the Pearl River.

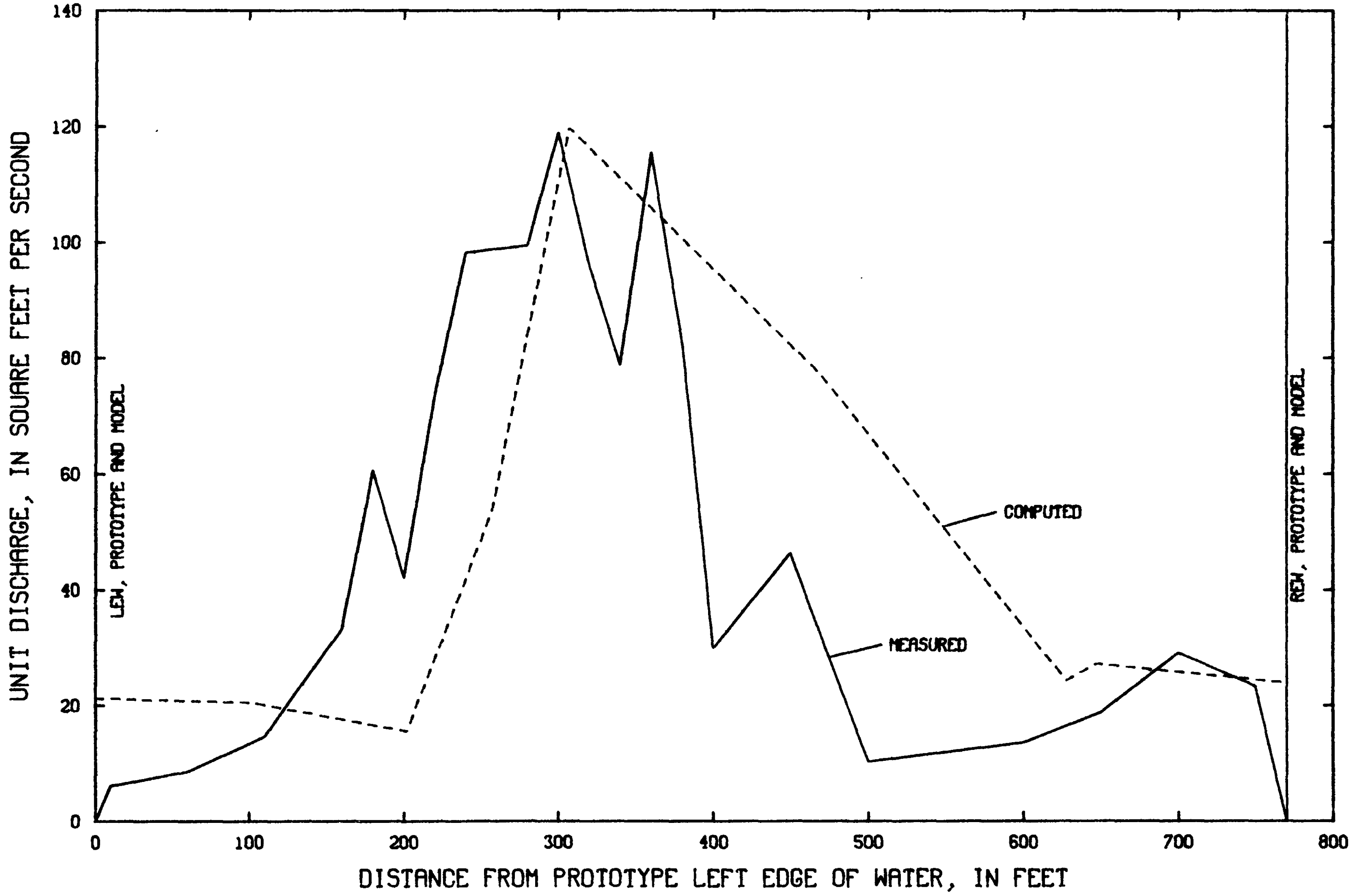

Figure 8.--Computed and measured unit discharge at the I-10 bridge opening at the Middle River.

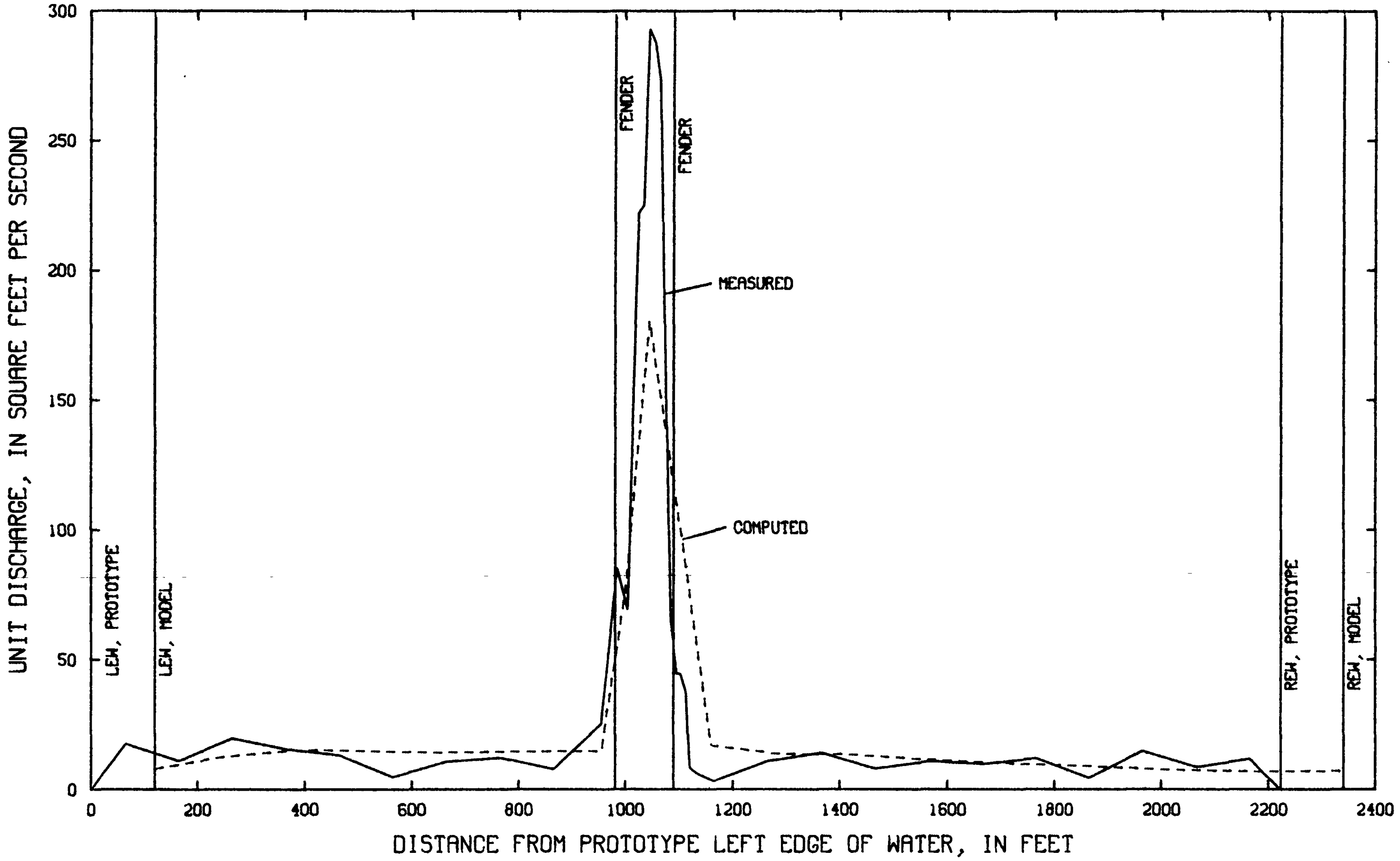

Figure 9.--Computed and measured unit discharge at the I-10 bridge opening at the West Pearl River.

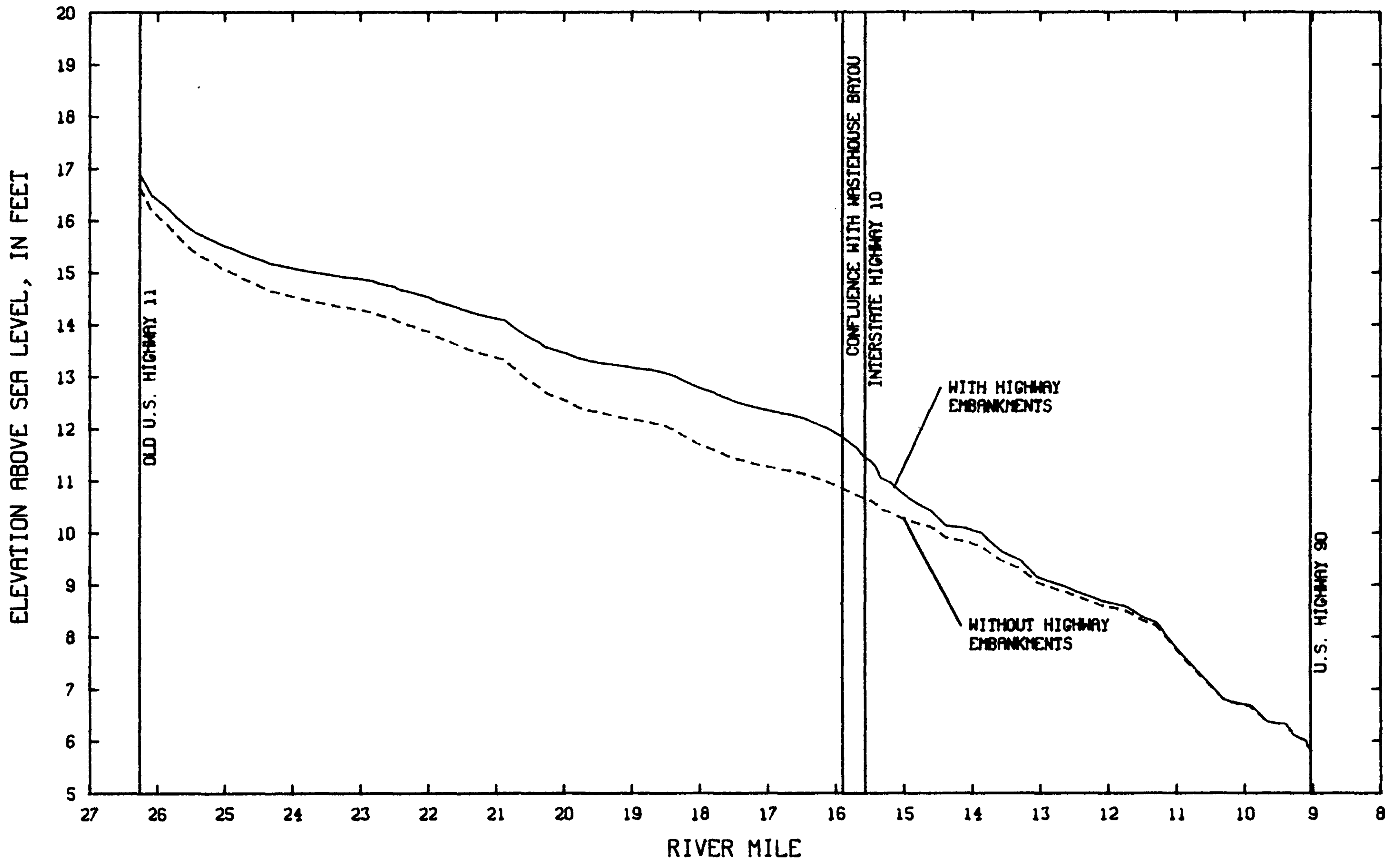

Figure 10.--Computed water-surface elevations for the Pearl River with and without the I-10 embankments in place.

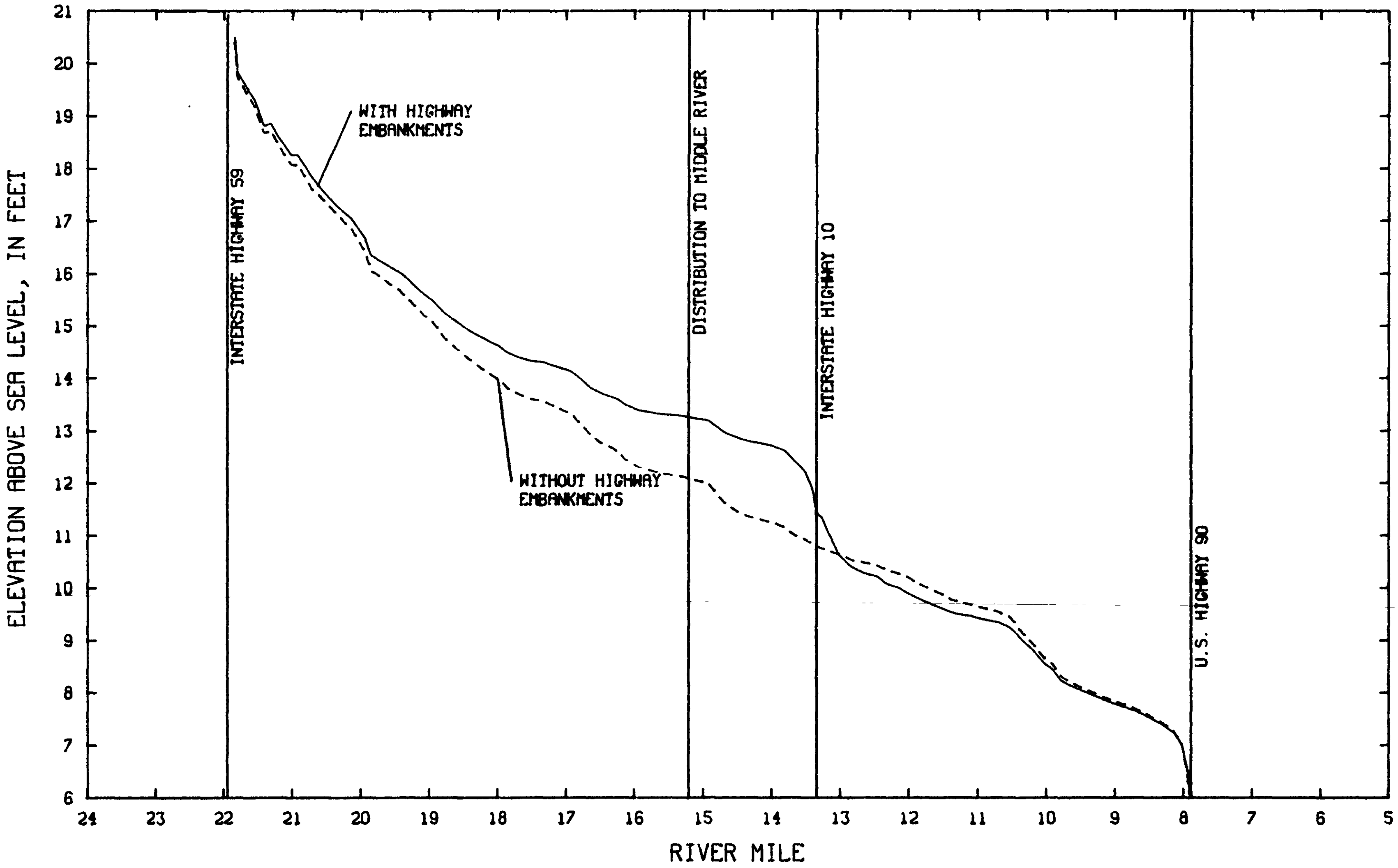

Figure 11.--Computed water-surface elevations for the West Pearl River with and without the I-10 embankments in place.

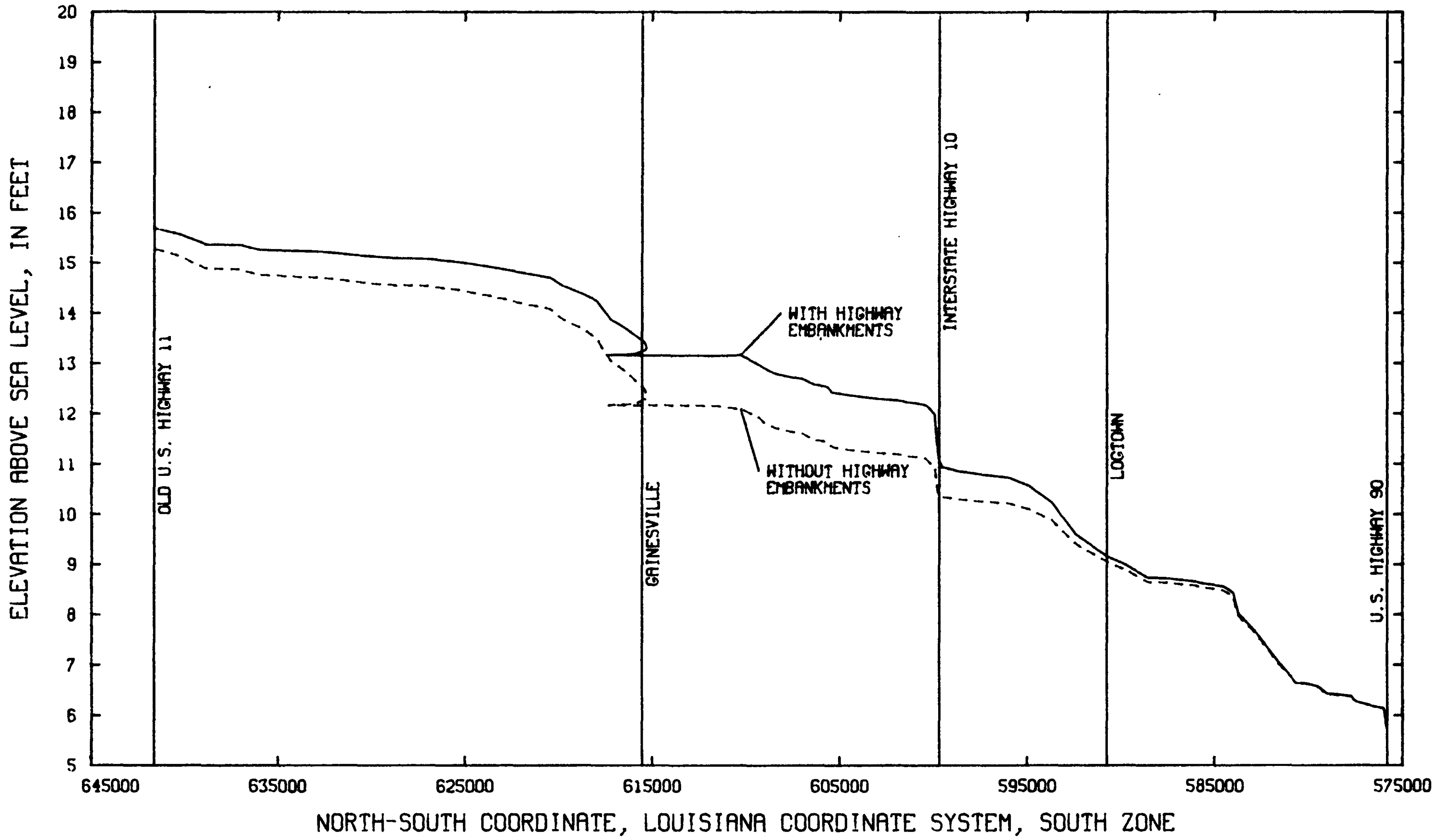

Figure 12.--Computed water-surface elevations at the east edge of the flood plain with and without the I-10 embankments in place.

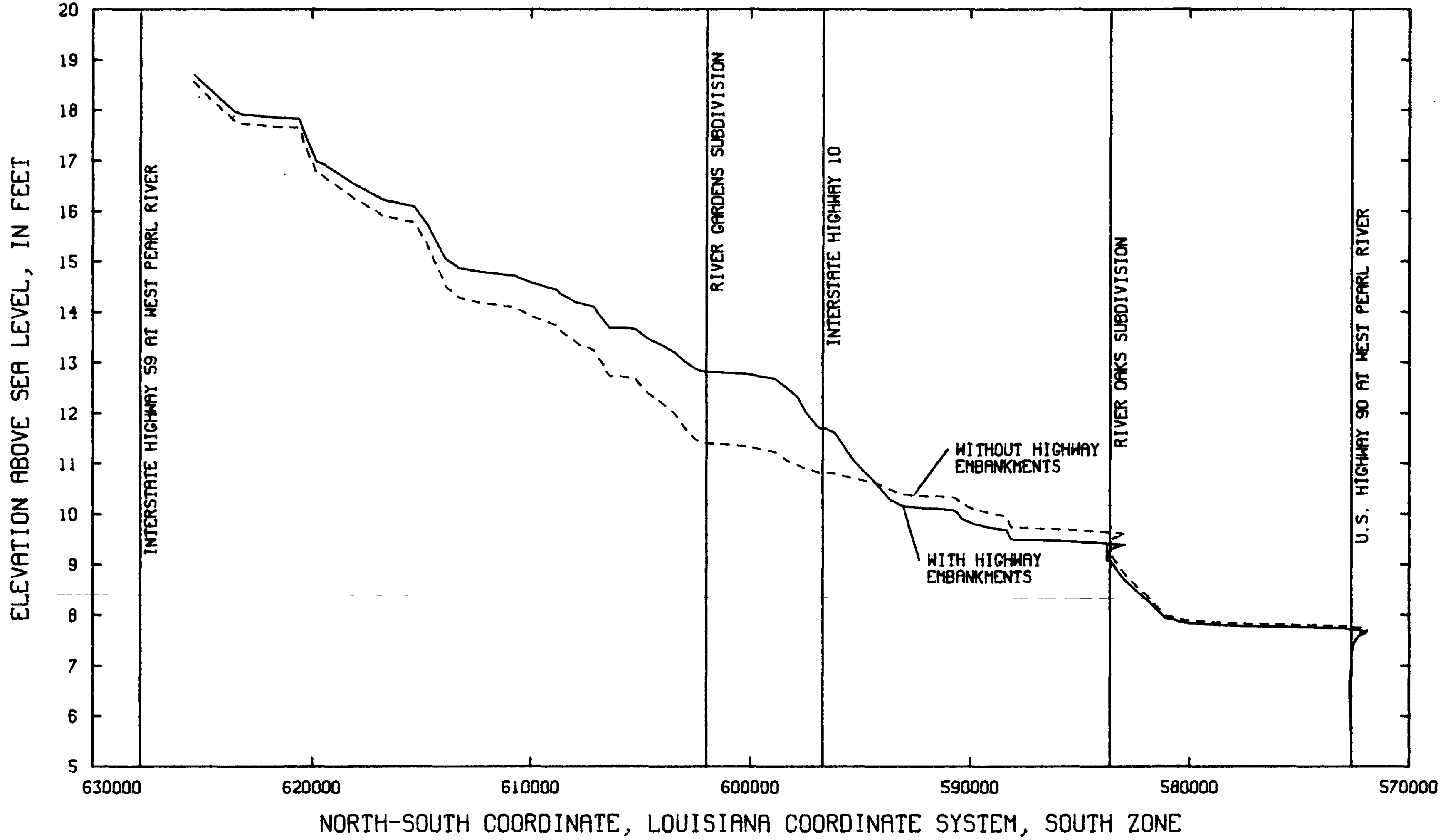

Figure 13.--Computed water-surface elevations at the west edge of the flood plain with and without the I-10 embankments in place.

Within a 3-mile-long reach centered about I-10, the flow converges toward and passes through the three bridge openings and then diverges back onto the flood plain. Along the upstream side of the I-10 embankments, the flow divides at approximately 71 percent of the way from the Pearl River to the Middle River and at approximately 64 percent of the way from the Middle River to the West Pearl River. Just downstream from I-10, the water surface is somewhat higher on the east side of the flood plain than on the west side. For example, 1 mi downstream from the roadway, the difference is about half a foot. Approximately 1.5 mi downstream from the highway crossing, the flow is again uniformly distributed across the flood plain, and the velocity field is aligned with the axis of the flood plain in a south-southeastward direction.

In an approximately mile-and-a-half-long reach upstream from Highway 90, the flow turns away from the flood-plain axis and moves in a southeastward direction. Along the upstream side of the Highway 90 embankments, the flow divides at approximately 60 percent of the way from the Pearl River to the East Middle River, at approximately 44 percent of the way from the East Middle River to the Middle River, at approximately 59 percent of the way from the Middle River to the West Middle River, and at approximately 63 percent of the way from the West Middle River to the West Pearl River. The water surface is about 1.5 ft higher at the west end of the Highway 90 crossing than at the east end. The computed discharges at the bridge openings in Highway 90 are given in table 8.

The contour lines shown on plate 2 indicate that water-surface gradients are largest at natural and man-made constrictions of the flood plain. Upstream from I-10, the slope of the water-surface in the direction of the axis of the flood plain is larger on the west side of the flood plain than on the east side. At I-10, the water-surface gradient is larger at the Middle River and West Pearl River openings than at the Pearl River opening. Downstream from I-10, the water-surface slope is generally larger on the east side of the flood plain than on the west side. At Highway 90, the water-surface gradient is much larger at the West Pearl River opening than at the other four openings.

Computed channel discharge for the Pearl and West Pearl Rivers is plotted as a function of river mile in figures 14 and 15, respectively. Throughout the study reach, except near the bridges, most of the discharge is in the flood plain. At the upstream boundary (river mile 26.3), the discharge in the channel of the Pearl River, with the I-10 embankments in place, is 22,000 ft^3/s. The discharge drops sharply downstream from old Highway 11 to a low of 2,760 ft^3/s at river mile 23.0. The discharge in the channel of the West Pearl River, with the I-10 embankments in place, drops from 69,100 ft^3/s at the upstream boundary (river mile 21.9) to 20,800 ft^3/s at river mile 20.9 and to 7,380 ft^3/s at river mile 18.2.

At the upstream boundary, 52 percent of the total discharge is in the channels of the Pearl and West Pearl Rivers. Less than 1.5 mi

Table 8.--Computed discharges at the Highway 90 bridge openings with and without the I-10 embankments in place

Bridge opening	With highway embankments		Without highway embankments	
	Discharge, in cubic feet per second	Discharge, as percent of total discharge	Discharge, in cubic feet per second	Discharge, as precent of total discharge
Pearl River	60,500	34.6	59,800	34.4
East Middle River	25,200	14.4	25,000	14.4
Middle River	27,600	15.8	27,500	15.8
West Middle River	32,000	18.3	32,100	18.4
West Pearl River	29,600	16.9	29,900	17.2
Total[1]	175,000	100	174,000	100

[1]The reason for the discrepancy between the total computed discharge and the total inflow is discussed on page 6.

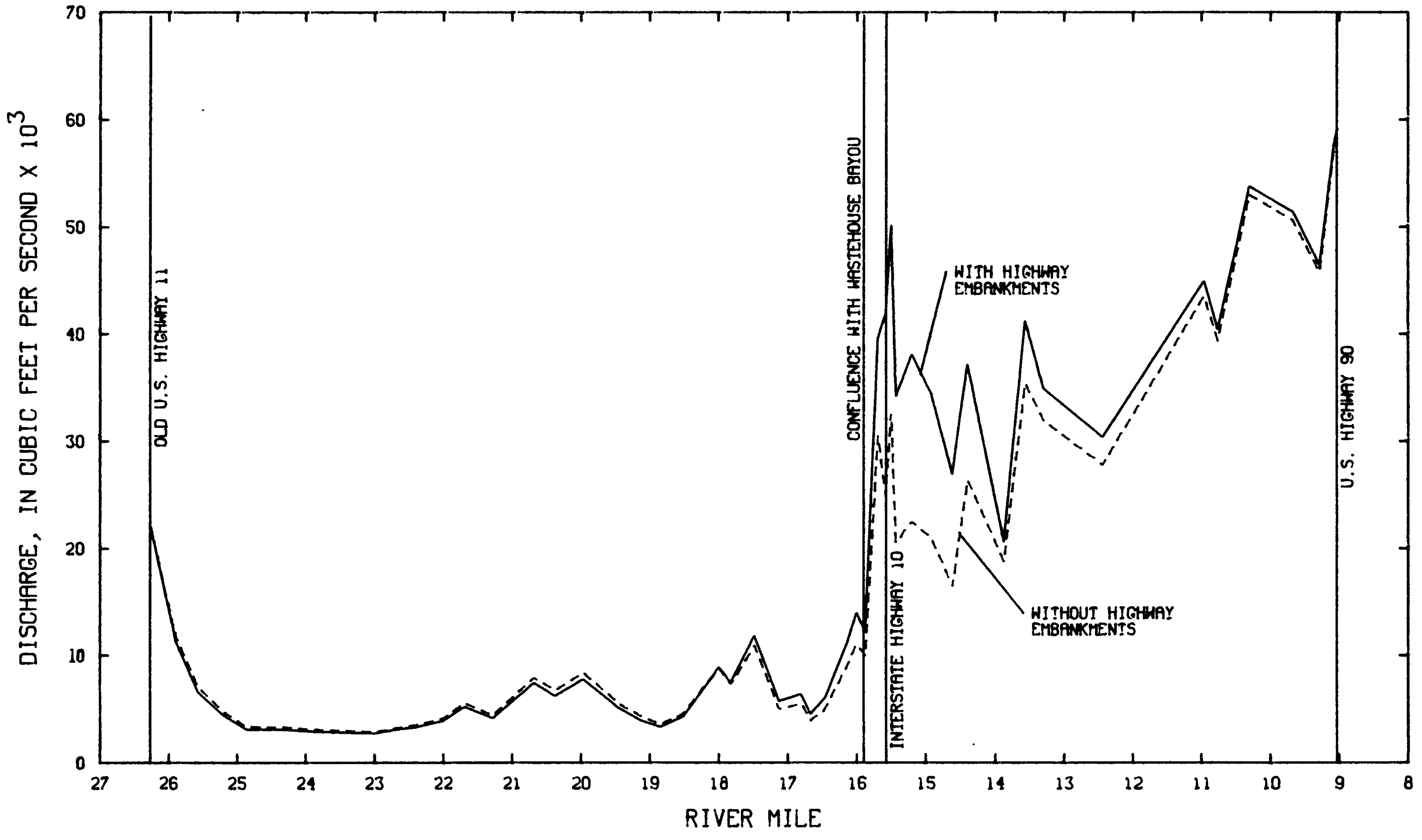

Figure 14.--Computed channel discharge for the Pearl River with and without the I-10 embankments in place.

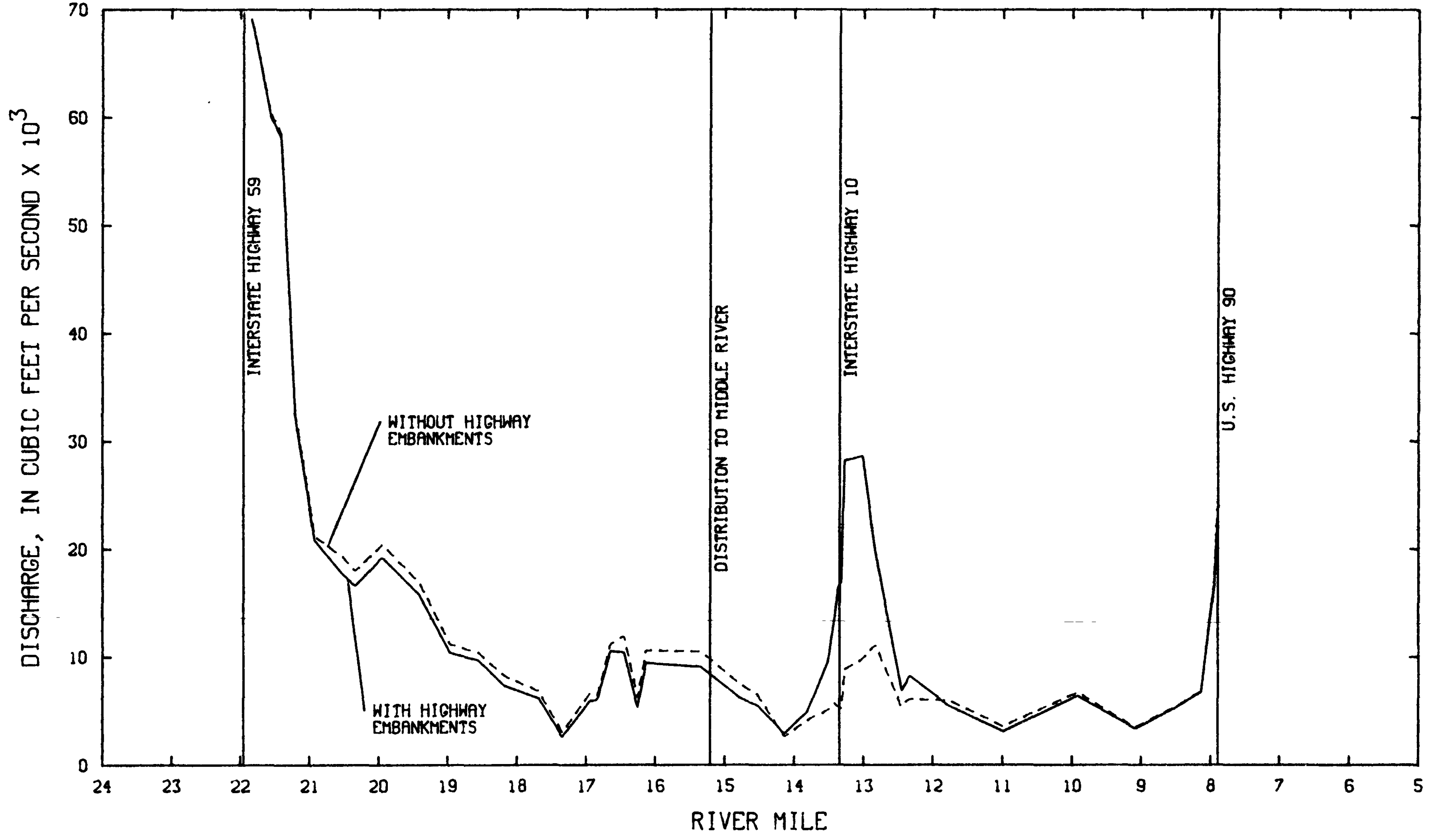

Figure 15.--Computed channel discharge for the West Pearl River with and without the I-10 embankments in place.

downstream, only 14 percent of the discharge is in the channels, and approximately halfway between the upstream boundary and I-10, only 6 percent of the discharge is in the channels. This value increases to 12 percent about a mile upstream from I-10 due to the increase in the number of channels from two to four. About 500 ft north of I-10, 36 percent of the discharge is in the three channels, and at the crossing, 49 percent of the computed discharge is in the channels. (Table 7 shows that 53 percent of the measured discharge was in the channels at I-10.)

In the reach from I-10 to Highway 90, between 25 and 41 percent of the discharge is in the channels. The increased channel discharge is due to both the increase in the size of the channel of the Pearl River downstream from Wastehouse Bayou and the increase in the number of channels. The discharge in the channel of the West Pearl River drops sharply at the downstream end of the widened reach between river miles 12.4 and 13.2. At the center of the reach (river mile 12.8), the channel discharge is 19,800 ft^3/s; at the downstream end, it is 6,920 ft^3/s. At Highway 90, 90 percent of the total discharge is in the five channels.

SIMULATION OF THE APRIL 2, 1980, FLOOD

WITHOUT THE I-10 EMBANKMENTS IN PLACE

The finite-element network used to simulate the April 2, 1980, flood was modified to represent conditions without I-10 in place, and the hydraulic impact of the I-10 embankments was determined by comparing results with and without I-10.

It should be noted that conditions with I-10 were compared to conditions without I-10, not to conditions prior to the construction of I-10. Thus, the reach of the West Pearl River between river miles 12.4 and 13.2, which was widened during construction, was not restored to its original width and depth in the simulation without I-10. However, because of the relatively small flow in the channel of the West Pearl River without I-10 in place, the difference with respect to backwater between conditions without I-10 and conditions prior to the construction of I-10 is almost certainly negligible.

Network Modifications

Elements were added in the areas occupied in the original network by the highway embankment between the Pearl and Middle Rivers, the embankment between the Middle and West Pearl Rivers, the 200-foot embankment at the left edge of the flood plain, and the knoll southeast of the West Pearl River bridge opening. Elsewhere, the two networks were identical.

Model ground-surface elevations at and near the highway embankments were changed where it was decided that they had been substantially altered during construction. Elevations ranging from 2.2 to 4.6 ft above sea level within the highway right-of-way on the right overbank at the Pearl River were lowered to 1.5 ft above sea level. No changes were made to ground-surface elevations on the left overbank. Elevations ranging from 2.5 to 4.0 ft above sea level on both overbanks at the Middle River were lowered to 2.0 ft above sea level. Ground-surface elevations on the right overbank at the West Pearl River were not changed, but elevations ranging from 4.0 to 9.0 ft above sea level on the left overbank were lowered to 2.5 ft above sea level. Elevations at and near the knoll southeast of the West Pearl River opening were lowered to the elevation of the surrounding flood plain, 1.5 to 3.0 ft above sea level, and elevations ranging from 5.0 to 8.0 ft above sea level between the knoll and the West Pearl River were lowered to between 3.0 and 5.0 ft above sea level. Natural levees along the channel banks were left in place.

The Chézy coefficients corresponding to the new elements and the elements formerly located in overbank areas under the I-10 bridges were assigned the value 22 $ft^{1/2}/s$, the value used in both simulations for the wooded flood plain (table 5). Upstream and downstream boundary conditions were the same as those used in the simulation with the highway embankments in place.

Results of the Simulation

The velocity field and water-surface contour lines for the simulation without I-10 in place are shown on plate 3. Computed water-surface elevation is plotted as a function of river mile for the channels of the Pearl and West Pearl Rivers in figures 10 and 11, respectively, and computed water-surface elevation is plotted for the east and west edges of the flood plain in figures 12 and 13, respectively.

Flow patterns in the upper and lower parts of the study reach are similar to those computed with the highway embankments in place. The discharges at the Highway 90 bridge openings are given in table 8. Throughout the middle part of the study reach, the flow is uniformly distributed across the flood plain and parallel to the flood-plain axis. In the reach extending from about 2 mi upstream from the site of I-10 to about a mile and a half upstream from Highway 90, the velocity field is aligned in a southward to south-southeastward direction.

As expected, water-surface elevations upstream from the I-10 site are lower without the highway embankments in place. Downstream from the roadway site, the water surface is lower on the east side of the flood plain and higher on the west side than it is with I-10 in place. There is no noticeable difference between water-surface elevations on opposite sides of the flood plain just downstream from the roadway site. Backwater caused by the I-10 embankments is discussed in detail in the next section.

Computed channel discharge for the Pearl and West Pearl Rivers is plotted as a function of river mile in figures 14 and 15, respectively. Throughout most of the reach upstream from the site of I-10, there is slightly more flow in the channels without the roadway in place. This is due to the lower water-surface elevations without the roadway. A decrease in water-surface elevations reduces cross-sectional flow areas more rapidly on the flood plain than in the channels. Only near the site of the highway crossing are channel discharges significantly lower. Approximately halfway between the upstream boundary and the site of I-10, 7 percent of the discharge is in the channels, compared with 6 percent with the roadway in place. About 500 ft north of the I-10 site, 22 percent of the discharge is in the channels, compared with 36 percent with the roadway present, and at the roadway site, 23 percent of the discharge is in the channels, compared with 49 percent with the roadway present. The percentages near the site of I-10 are larger than upstream values due to the increase in the size of the channel of the Pearl River downstream from Wastehouse Bayou and the increase in the number of channels.

Discharges in the three channels near the highway crossing were compared with and without the embankments in place. The discharge with the roadway in place is at least 30 percent higher than the discharge without the roadway in place from about 1,000 ft upstream from the crossing to about 7,000 ft downstream from the crossing in the channel of the Pearl River, from about 4,000 ft upstream to about 3,000 ft downstream in the channel of the Middle River, and from about 2,000 ft upstream to about 5,000 ft downstream in the channel of the West Pearl River.

Computed discharges at the site of I-10 with and without the highway embankments in place are given in table 9. Without the highway embankments in place, flow is reduced 41 percent at the Pearl River bridge opening, 80 percent at the Middle River opening, and 67 percent at the West Pearl River opening. Without the roadway in place, the computed discharge across that part of the flood plain that is occupied by the embankments with the roadway present is 95,200 ft^3/s. With the roadway in place, 48 percent of this discharge is added to the discharge at the Pearl River opening, 23 percent to the discharge at the Middle River opening, and 27 percent to the discharge at the West Pearl River opening. (The 2-percent discrepancy is due to a conservation-of-mass error, which occurs for the reason discussed on page 6.) Thus, without I-10 in place, the flow shift from the west side of the flood plain to the east side is reduced upstream from the site of I-10.

In the reach downstream from the site of I-10, between 20 and 41 percent of the discharge is in the channels. The discharge at the widened reach of the West Pearl between river miles 12.4 and 13.2 drops from 11,100 ft^3/s at the center of the reach (river mile 12.8) to 5,420 ft^3/s at the downstream end. From a mile downstream from the site of I-10 to Highway 90, the discharge in the channel of the West Pearl River is virtually the same with and without the highway embankments in place. At Highway 90, 91 percent of the total discharge is in the channels.

Table 9.--Computed discharges at I-10 with and without the I-10 embankments in place

Subsection	Discharge with highway embankments, in cubic feet per second	Discharge without highway embankments, in cubic feet per second
Embankment between left edge of flood plain and Pearl River.	0	833
Pearl River, left overbank	23,600	13,800
Pearl River, channel	50,200	32,500
Pearl River, right overbank	36,100	18,100
Pearl River, total	110,000	64,400
Embankment between Pearl and Middle Rivers.	0	29,900
Middle River, left overbank	3,810	916
Middle River, channel	17,800	3,320
Middle River, right overbank	5,360	1,100
Middle River, total	27,000	5,340
Embankment between Middle and West Pearl Rivers.	0	64,500
West Pearl River, left overbank	10,000	3,560
West Pearl River, channel	16,900	5,260
West Pearl River, right overbank	11,000	3,580
West Pearl River, total	37,900	12,400
Total1/	175,000	177,000

1/The reason for the discrepancy between the total computed discharge and the total inflow is discussed on page 6.

Backwater and Drawdown Caused by the I-10 Embankments

A map of backwater and drawdown was obtained by subtracting nodal water-surface elevations computed without the roadway in place from the corresponding nodal water-surface elevations computed with the roadway in place. Lines of equal backwater and drawdown are shown on plate 4. Backwater and drawdown are plotted as a function of river mile for the channels of Pearl and West Pearl Rivers in figure 16, and values of backwater or drawdown at locations of interest are given in table 10.

When highway embankments are removed in a flood-plain model, error in the computed water surface due to incorrect simulation of the fall through bridge openings is also removed. Hence, backwater, which is computed by subtracting the water surface without highway embankments in place from the water surface with embankments in place, still contains this error. On the other hand, when highway embankments are removed, error due, for example, to incorrect values of flood-plain Chézy coefficients is still present in the computed water surface. Much of this error cancels when the water surface computed without the highway in place is subtracted from the water surface computed with the highway in place. Thus, error in computed backwater is likely to be less than error in the calibrated water surface computed with highway embankments in place.

The 1.2-foot to 2.0-foot lines form a "mound" north of I-10 between the Pearl River and the west edge of the flood plain. The 0.2-foot to 1.0-foot lines are aligned approximately in a southwest-to-northeast direction. Although maximum backwater at the west edge of the flood plain (1.5 ft) is greater than maximum backwater at the east edge (1.1 ft), backwater decreases more rapidly in the upstream direction along the west edge of the flood plain than along the east edge.

Backwater ranging from 0.6 to 0.2 ft extends more than a mile downstream from the Pearl River bridge opening in I-10 at the east edge of the flood plain. A large area of drawdown extends from the downstream side of the highway embankment between the Middle and West Pearl Rivers to the west edge of the flood plain. Drawdown of 0.2 ft or more occurs along approximately 2 mi of the west edge of the flood plain downstream from I-10.

DISCUSSION

A combination of natural and man-made factors causes most of the flow to enter the study reach on the west side of the flood plain and leave on the east side (tables 1 and 8). The ground-surface contour lines between the upstream model boundary and I-10 show that ground-surface elevations are higher near the West Pearl River than on the east side of the flood plain (pl. 1). At the upstream boundary, the channel of the West Pearl River is larger than the channel of the Pearl River. South of its confluence with Wastehouse Bayou, the channel of the Pearl River is much larger than that of the West Pearl River. The Middle River and Wastehouse

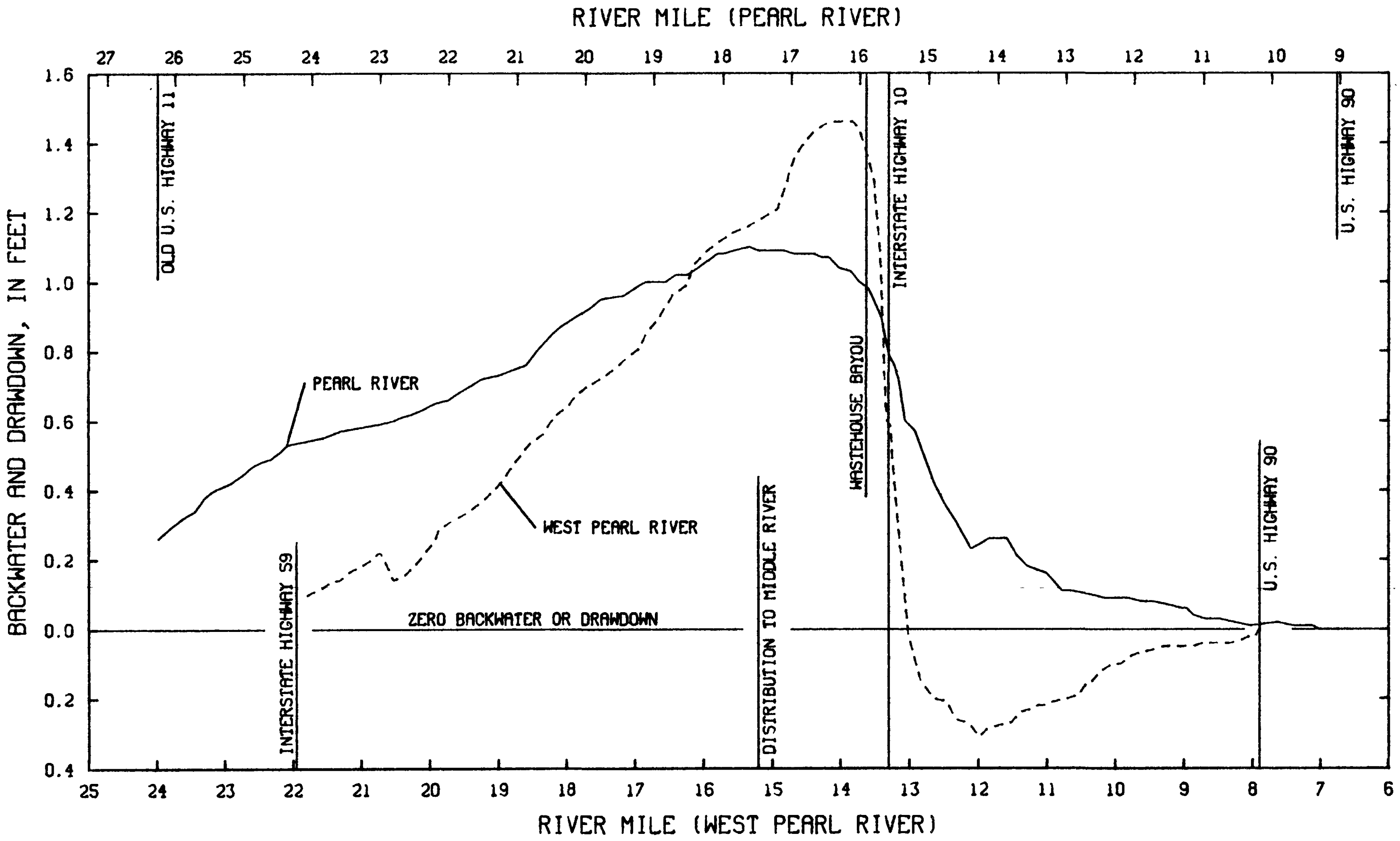

Figure 16.--Computed backwater and drawdown for the Pearl and West Pearl Rivers.

Table 10.--Computed water-surface elevations with and without the I-10 embankments in place and backwater or drawdown

Location reference number1/	Location	Water-surface elevation above sea level with highway embankments, in feet	Water-surface elevation above sea level without highway embankments, in feet	Backwater or drawdown2/, in feet
1	Old Highway 11 at east edge of flood plain.	15.7	15.3	0.4
2	Gainesville	13.3	12.4	0.9
3	Napoleon	12.8	11.7	1.1
4	Location of maximum backwater at east edge of flood plain.	12.6	11.5	1.1
5	Logtown	9.2	9.1	0.1
6	Location of maximum backwater on north side of embankment between Pearl and Middle Rivers.	12.4	10.6	1.8
7	Location of maximum drawdown on south side of embankment between Pearl and Middle Rivers.	10.5	10.6	(0.1)
8	Old Highway 11 at Pearl River.	16.9	16.6	0.3
9	Location of maximum backwater on north side of the embankment between Middle and West Pearl Rivers.	12.7	10.6	2.1
10	Location of maximum drawdown on south side of embankment between Middle and West Pearl Rivers.	10.0	10.7	(0.7)
11	I-59 at West Pearl River.	20.5	20.4	0.1

Table 10.--Computed water-surface elevations with and without the I-10 embankments in place and backwater or drawdown--Continued

Location reference number[1]	Location	Water-surface elevation above sea level with highway embankments, in feet	Water-surface elevation above sea level without highway embankments, in feet	Backwater or drawdown[2], in feet
12	Porters River Landing	17.0	16.8	0.2
13	Magnolia Forest Subdivision, northeast corner.	14.8	14.2	0.6
14	Morgan Bluff	14.2	13.4	0.8
15	Davis Landing	13.8	12.9	0.9
16	River Gardens Subdivision	12.8	11.4	1.4
17	Mouth of Gum Bayou	12.7	11.3	1.4
18	Location of maximum backwater at west edge of flood plain.	12.7	11.2	1.5
19	Location of maximum drawdown at west edge of flood plain.	9.9	10.2	(0.3)
20	Quail Ridge Subdivision	9.8	10.1	(0.3)
21	River Oaks Subdivision, north side.	9.3	9.5	(0.2)

1/Location reference numbers are shown on plate 4.
2/Values of drawdown are given in parentheses.

Bayou cross the flood plain diagonally from west to east. At high stages, these topographic factors cause water to flow across the flood plain from the higher west side to the lower east side either with or without I-10 in place. However, with the roadway in place, the shift of flow from west to east occurs farther upstream. (See pls. 2 and 3.)

Accompanying the roadway-induced shift of flow to the east are higher water-surface elevations downstream from the roadway in the eastern part of the flood plain and lower water-surface elevations downstream in the western part. Upstream from the roadway, maximum backwater at the west edge of the flood plain is greater than maximum backwater at the east edge. However, because of the larger water-surface slope on the west side of the flood plain, backwater decreases more rapidly in the upstream direction along the west edge than along the east edge. (See pl. 4.)

For the three discharge measurements made at I-10 in 1979 and 1980, between 59 and 61 percent of the total discharge was at the Pearl River bridge opening (table 1). For the April 2, 1980, flood, about half of the discharge across the sites of the highway embankments without the roadway in place is diverted to the Pearl River opening when the roadway is in place (table 9). The change in the flow distribution and the lateral variations in backwater and drawdown with I-10 in place are due in part to the greater constriction of the flow in the western part of the flood plain than in the eastern part and in part to the topography of the flood plain.

The results obtained in this study suggest that the parallel I-59 and Southern Railroad embankments just north of the study reach and the Highway 90 embankments at the south end of the study reach may have significant hydraulic effects within and near the study area. The large proportion of the total flow entering the study reach at the West Pearl River (table 1) and the water-surface "mound" just downstream from the I-59 bridge opening at the West Pearl River (pl. 2) suggest that the I-59 and Southern Railroad embankments may contribute to a westward shift of flow upstream from I-59 and may cause backwater downstream from I-59. Observations made while adjusting the upstream discharge distribution and discussed on pages 29 and 30 suggest that such backwater extends no more than 3 or 4 mi downstream from I-59. An upstream extension of the finite-element network of about 5 mi would be needed to quantify the hydraulic effect of I-59 and the Southern Railroad.

Several factors discussed on page 45 suggest that backwater upstream from Highway 90 may be greater on the west side of the flood plain than on the east side: (1) Highway 90 constricts the western part of the flood plain more than the eastern part, (2) there is an eastward flow shift just upstream from the roadway, (3) water-surface elevations are higher at the west end of Highway 90 than at the east end, and (4) the water-surface gradient in the downstream direction is much larger at the West Pearl River bridge opening than at the other openings. A downstream extension of the finite-element network of about 2 mi would be needed to quantify the hydraulic effect of Highway 90.

SUMMARY AND CONCLUSIONS

The two-dimensional finite-element surface-water flow modeling system FESWMS was used to study the effect of I-10 on water-surface elevations and flow distribution during the April 2, 1980, flood on the Pearl River near Slidell, La. A finite-element network was designed to represent the topography and vegetative cover of the study reach. Hydrographic data collected for the April 2, 1980, flood were used to adjust the flow model to simulate the flood as closely as possible. The finite-element network was then modified to represent conditions without I-10 in place, and the hydraulic impact of I-10 was determined by comparing results with and without I-10.

Without I-10 in place, much of the flow shifts from the west side of the flood plain to the east side upstream from the site of I-10. With I-10 in place, this flow shift occurs farther upstream than it does without the roadway in place. Upstream from the roadway, maximum backwater at the west edge of the flood plain (1.5 ft) is greater than maximum backwater at the east edge (1.1 ft), but backwater decreases more rapidly in the upstream direction along the west edge of the flood plain than along the east edge. Backwater ranging from 0.6 to 0.2 ft extends more than a mile downstream from the Pearl River bridge opening in I-10 at the east edge of the flood plain, and drawdown of 0.2 ft or more occurs along approximately 2 mi of the west edge of the flood plain downstream from I-10.

The results of the study suggest that I-59, the Southern Railroad, and Highway 90 may have significant hydraulic effects in and near the study reach. Further work would be needed to quantify these effects.

The capability of the modeling system FESWMS to simulate the significant features of steady-state flow in a complex multichannel river-flood-plain system with variable topography and vegetative cover was successfully demonstrated in this study. These features included lateral variations in discharge distribution, water-surface elevation, and backwater or drawdown at and near I-10, caused in part by the greater constriction of the flow in the western part of the flood plain and in part by the topography of the flood plain.

REFERENCES

Cardwell, G. T., Forbes, M. J., Jr., and Gaydos, M. W., 1967, Water resources of the Lake Pontchartrain area, Louisiana: Baton Rouge, La., Louisiana Department of Conservation, Geological Survey, and Louisiana Department of Public Works, Water Resources Bulletin No. 12, 105 p.

Chow, V. T., 1959, Open-channel hydraulics: New York, McGraw-Hill, 680 p.

Gee, D. M., and MacArthur, R. C., 1978, Development of generalized free surface flow models using finite element techniques, in Brebbia, C. A., and others, eds., Finite elements in water resources: International Conference on Finite Elements in Water Resources, 2nd, London, 1978, Proceedings: London, Pentech Press, p. 2.61-2.79.

Hood, P., 1976, Frontal solution program for unsymmetric matrices: International Journal for Numerical Methods in Engineering, v. 10, no. 2, p. 379-399.

_____ 1977, Note on frontal solution program for unsymmetric matrices: International Journal for Numerical Methods in Engineering, v. 11, no. 6, p. 1055.

King, I. P., and Norton, W. R., 1978, Recent applications of RMA's finite element models for two dimensional hydrodynamics and water quality, in Brebbia, C. A., and others, eds., Finite elements in water resources: International Conference on Finite Elements in Water Resources, 2nd, London, 1978, Proceedings: London, Pentech Press, p. 2.81-2.99.

Lee, F. N., and Arcement, G. J., 1981, Hydrologic analysis of Pearl River floods, April 1979 and April 1980, in Louisiana and Mississippi: Baton Rouge, La., Louisiana Department of Transportation and Development, Office of Highways, 37 p.

Lee, J. K., 1980, Two-dimensional finite element analysis of the hydraulic effect of highway bridge fills in a complex flood plain, in Wang, S. Y., and others, eds., Finite elements in water resources: International Conference on Finite Elements in Water Resources, 3rd, University, Miss., 1980, Proceedings: University, Miss., University of Mississippi, School of Engineering, p. 6.3-6.23.

Lee, J. K., and Bennett, C. S., III, 1981, A finite-element model study of the impact of the proposed I-326 crossing on flood stages of the Congaree River near Columbia, South Carolina: U.S. Geological Survey Open-File Report 81-1194, 56 p.

Norton, W. R., and King, I. P., 1973, A finite element model for Lower Granite Reservoir. Computer application supplement and user's guide: Walnut Creek, Calif., Water Resources Engineers, Inc., 90 p.

Norton, W. R., King, I. P., and Orlob, G. T., 1973, A finite element model for Lower Granite Reservoir: Walnut Creek, Calif., Water Resources Engineers, Inc., 138 p.

Pinder, G. F., and Gray, W. G., 1977, Finite element simulation in surface and subsurface hydrology: New York, Academic Press, 295 p.

Pritchard, D. W., 1971, Two-dimensional models, in Ward, G. H., Jr., and Espey, W. H., Jr., eds., Estuarine modeling: An assessment: Washington, D.C., Environmental Protection Agency, Water Quality Office, Water Pollution Control Research Ser. 16070DZV, p. 22-33.

Shell, J. D., 1981, Drainage areas in the Pearl River basin, Mississippi-Louisiana. Part 2. Pearl River below Strong River to mouth: U.S. Geological Survey, 232 p.

Tseng, M. T., 1975, Evaluation of flood risk factors in the design of highway stream crossings. V. III. Finite element model for bridge backwater computation: Washington, D.C., Federal Highway Administration, Report No. FHWD-RD-75-53, 176 p.

U.S. Army Corps of Engineers, 1981, Pearl River basin reconnaissance report (stage 1 report): Mobile, Ala., U.S. Army Corps of Engineers, 200 p.

U.S. Geological Survey, 1981, Water resources data for Mississippi: U.S. Geological Survey Water-Data Report MS-79-1, 438 p.

_____ 1982, Water resources data for Louisiana. V. 2. Southern Louisiana: U.S. Geological Survey Water-Data Report LA-81-2, 327 p.

U.S. Water Resources Council, 1977, Guidelines for determining flood flow frequency: Washington, D.C., U.S. Water Resources Council, Hydrology Committee, Revised Bulletin 17A, 163 p.

Walters, R. A., and Cheng, R. T., 1978, A two-dimensional hydrodynamic model of a tidal estuary, in Brebbia, C. A., and others, eds., Finite elements in water resources: International Conference on Finite Elements in Water Resources, 2nd, London, 1978, Proceedings: London, Pentech Press, p. 2.3-2.21.

_____ 1980, Accuracy of an estuarine hydrodynamic model using smooth elements: Water Resources Research, v. 16, no. 1, p. 187-195.

Wax, C. L., and Tingle, J. L., 1980, The Pearl River flood of Easter 1979: A water balance explanation: Mississippi State, Miss., Mississippi State University, Water Resources Research Institute, 27 p.

Zienkiewicz, O. C., 1977, The finite element method (3rd ed.): London, McGraw-Hill, 787 p.